Earth-Science Reviews 272 (2026) 105324

Contents lists available at ScienceDirect

Earth-Science Reviews

journal homepage: www.elsevier.com/locate/earscirev

Nickel: Geochemistry, biochemistry and its role in chemical and biological evolutions

Anna Neubeck [a,b], Andreas Kirschning [c,d,*]

[a] Department of Earth Sciences, Uppsala University, Villavägen 16, 752 36 Uppsala, Sweden
[b] Department of Soil and Environment, Swedish University of Agricultural Sciences, Lennart Hjelms väg 9, Uppsala, Sweden
[c] Institute of Organic Chemistry, Leibniz University Hannover, Schneiderberg 1B, 30167 Hannover, Germany
[d] Uppsala Biomedical Center (BMC), Uppsala University, Husargatan 3, 752 37 Uppsala, Sweden

ARTICLE INFO

Keywords:
Biochemistry
Geochemistry
Nickel
Origin of life
Prebiotic chemistry

ABSTRACT

Nickel is a versatile element that plays critical roles in Earth's geological and biological evolution, from the depths of the magmatic mantle to the complexity of prebiotic chemistry. While it is not considered the sole catalyst for the origin of life, recent research suggests that Ni may have had a more profound role than traditionally recognized. This review synthesizes Ni isotope geochemistry, biology, and prebiotic chemistry, exploring how Ni isotope variations offer new insights into magmatic processes, hydrothermal systems, and the cycling of Ni through Earth's lithosphere and hydrosphere. We summarize the pathways of Ni in oceanic environments, highlighting its influence on biogeochemical cycles and microbial metabolisms that shape global ecosystems. Furthermore, we examine the essential roles of Ni in biological systems, focusing on its function as a catalytic metal in enzymes crucial for nitrogen and carbon cycling. Extending to the prebiotic world, we evaluate Ni's potential in catalyzing life's earliest chemical reactions, including the polymerization of amino acids and the fixation of CO_2, possibly driven by unique metal-ligand interactions. Our comprehensive review positions Ni as a pivotal element across geological timescales and environments, underscoring its relevance to both planetary and biochemical processes.

Contents

* Corresponding author at: Institute of Organic Chemistry, Leibniz University Hannover, Schneiderberg 1B, 30167 Hannover, Germany.
E-mail addresses: anna.neubeck@geo.uu.se (A. Neubeck), andreas.kirschning@oci.uni-hannover.de (A. Kirschning).

https://doi.org/10.1016/j.earscirev.2025.105324
Received 9 April 2025; Received in revised form 2 November 2025; Accepted 6 November 2025
Available online 8 November 2025

1. Introduction

A simplistic view of life could describe it as a fixed set of instructions linked to a machinery. Today's DNA code corresponds to the instructions and these represent the development of life in coded form from its origin to the present. In his remarkable 1997 article, William argued that the code cannot be the source of evolution. This code is inherently conservative (Williams, 1997) and DNA damage, externally induced by physical and chemical stress, led to the evolutionary development we know. In essence, the conservatism of DNA resists these changes, regardless of the option that progress may be possible as a result. In this context, the availability of energy and material is a particular aspect that contributes to the ability of organisms to survive. One may paint a different initial picture, but the availability of chemical elements on the early Earth was a basic prerequisite for chemical and eventually biological evolution to become possible. Geochemical activities led to environmental changes and influenced the viability of existing life forms. However, once large parts of the earth were colonized, these also had feedback effects on the geosphere and thus on the availability of resources (Fig. 1).

Discussion on the emergence of life from a geochemical environment as well as experiments on prebiotic chemistry put the metal Fe in particular focus, while Ni has been given a more marginal role. For many reasons, this bias is not entirely justified, considering the special catalytic and geometric properties of the metal and also its importance in central biochemical and metabolic processes. This is especially the case for anaerobic organisms and these are thought to have appeared early in evolution (Alfano & Cavazza). According to Ananakov and his reference to P. Sabatier: Nickel is *The "Spirited Horse" of Transition Metal Catalysis* (Ananikov, 2015; Sabatier, 1922) the importance of Ni is associated with its abundance on planet earth and its particular involvement in catalysis with gases such as H_2 and CO. The metal is therefore a top candidate to be dealt with in the context of evolution and the emergence of life. Here, we wish to emphasize the unique importance of Ni for the appearance of life on Earth, its involvement in geo-biochemical cycles and its biochemistry. Finally, we try to place the role of this metal in the context of prebiotic chemistry and above all of biochemical systems embedded in an evolutionary context.

2. Nickel geochemistry

2.1. Origin on planet earth

Nickel with the atomic number 28 is the fifth most common element on earth. Along with a few other transition metals it is essential for most forms of life. Its name comes from a mischievous imp of German mining mythology called Ni, for Ni minerals were green as well as copper ores and were therefore called copper Ni because they did not yield copper. Five stable isotopes (^{58} Ni, ^{60}Ni, ^{61}Ni, ^{62} Ni and ^{64} Ni) of naturally occurring Ni are known with ^{58}Ni being the most abundant one. The metal is formed through nucleosynthesis through fusion (up to ^{56}Ni) and neutron capture (all isotopes heavier than ^{56}Ni). Nucleosynthesis is a process which describes the creation of chemical elements by nuclear fusion or neutron capture within stars or dying stars (Clayton et al., 1961; Clayton, 1983). In particular, it is thought that the higher-density ejecta of white dwarfs favours the synthesis of stable isotopes of Ni (Blondin 2022).

Around 95% of the Ni found in the bulk silicate Earth (BSE) is believed to have originated from late-stage planetary impacts, including the giant impact that formed the Moon and the Late Veneer event. These impacts played a crucial role in delivering significant amounts of Ni to the Earth's interior. Interestingly, over 95% of meteorites are composed

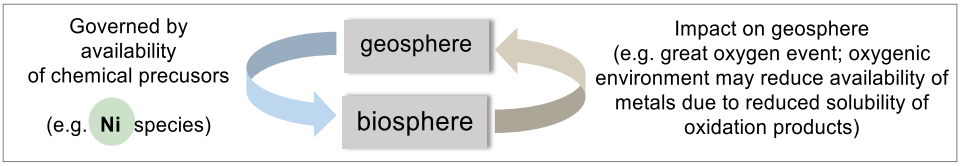

Fig. 1. The tight interplay and influence between the geosphere and biosphere with regard to the availability of chemical species including metals such as Ni.

of Fe-Ni (FeNi) alloys, which contain between 5% and 30% Ni. This makes meteorites an exceptionally rich source of Ni, with concentrations far exceeding those found in nearly any terrestrial rock. Consequently, the elevated Ni content in meteorites has been key in shaping the Earth's current Ni distribution, particularly through these impact events. Even though these impactors only contributed to 35% of Earths total mass, an overwhelming amount of the total Ni budget was delivered during these times and was distributed preferentially into mantle olivine (Wang et al. 2021). However, stable Ni isotope analyses show that there is a difference between the lighter (+0.10 ‰) average BSE and the heavier (+0.23 ‰) average chrondritic material, suggesting either an isotopic fractionation due to the earth's differentiation or addition of another, non-chondritic Ni source. However, molecular dynamic simulations on the isotopic fractionation difference between Fe Ni sulfide and magnesium Ni silicate melt phases show a very small isotopic difference. Alternative hypotheses, such as the Moon-forming impact, evaporative loss, collision erosion, and core-mantle chemical diffusion, have been ruled out through mass balance calculations (Wang et al., 2021; Klaver et al., 2020). Instead, the observed discrepancy in isotopic composition is more plausibly explained by the impact and subsequent accretion of a sulfide-rich, highly reduced planetary body. This scenario suggests that a body with these specific characteristics contributed to the Earth's unique isotopic signature, offering a more plausible explanation than previously considered processes. Since rocks with a high S/Si ratio have significantly lighter δ^{60}Ni values (Gueguen et al., 2013, Hofmann et al. 2014), a S-rich impactor may explain the discrepancies. This illustrates the strong affinities between Ni and S, which is evident also throughout the history of geochemistry and biology.

2.2. Geochemical occurrence

Nickel naturally occurs on Earth in the forms of Ni oxides, Ni sulfides, and Ni silicates (Galoisy, 1998). It is most abundant in the Earth's core, where it makes up approximately 8% of the total composition, while in the crust, it is present in much smaller quantities, around 0.01%. These varying concentrations reflect the element's distribution within the Earth, with a significant portion being concentrated in the deep interior. (Walsh and Orme-Johnson, 1987). Abundant Ni containing sulfide ores are pentlandite [$(Ni,Fe)_9S_8$], Ni magnetite [$(Fe^{2+},Ni)Fe_2^{3+}O_4$], and some other Ni minerals such as millerite (NiS) as well as nickelite (NiAs) and nickeliferous pyrrhotite ($(Fe,Ni)_9S_8$. Other sources are lateritic Ni ores, mainly from garnierite, a mixture of népouite ($Ni_3Si_2O_5(OH)$) and willemseite ($(Ni,Mg)_3Si_4O_{10}(OH)_2$). Approximately 70% of the world's Ni resources are found in serpentinitic, lateriric soils, which are strongly fractionated due to preferential adsorption onto clays, Fe and manganese oxyhydroxides (Machado et al., 2023). In fact, more than 200 Ni-containing minerals are known today, and many of them were already present on the prebiotic earth (Hazen et al. 2008). During the prebiotic era, planetary accretion delivered a foundational suite of minerals, including metallic, sulfidic, phosphatic minerals. These initial mineral phases were gradually transformed and diversified through processes associated with crustal formation (4.55 to 2.5 Ga), leading to the emergence of the diverse set of magmatic, metamorphic and sedimentary minerals that we have today. Most of the Ni on Earth was indeed delivered during the early planetary accretion phase and became part of the core and mantle. The diversification of Ni-bearing minerals at the time of crustal formation include the formation of Fe-Ni sulfides and hydroxides formed through hydrothermal processes, volcanism and a dawning anaerobic biological world (Hazen et al. 2008, Mielke et al. 2010, 2011). In a model for the origin of life, it is proposed that hydrogen sulfide anions interact with oceanic Fe, Ni, and cobalt to precipitate catalytic sulfide-bearing compounds crucial for the onset of life. These compounds, consisting of Ni-Fe sulfides, are believed to have formed in the early earth's oceans with transition metals like Ni deriving from acidic hydrothermal fluids.

Nickel can adopt multiple oxidation states (−1, 0, +1, +2, +3, +4), but in both geochemical and biological contexts the divalent form Ni(II) overwhelmingly dominates. This is because the electronic configuration of Ni (with a partially filled d-shell) lends itself to a stable divalent state that combines manageable electron-removal energy with favourable ligand-field interactions (Alfano and Cavazza, 2020; Siegbahn et al., 2019). In contrast, iron more readily cycles between Fe(II) and Fe(III), which underpins much of its role in biological redox chemistry (Liu et al., 2024). In many aqueous or biological environments, oxidation of Ni(II) to Ni(III) is rarely accessible without specialised ligand scaffolds or oxidising conditions, because Ni binds its d electrons more tightly and lacks the facile one-electron redox transitions found in iron systems (Siegbahn et al., 2019). In enzymes such as urease and [NiFe]-hydrogenase, this coordination-based mode of catalysis is clearly observed, with nickel remaining in a stable divalent state rather than shifting into higher oxidation states (Alfano and Cavazza, 2020; Siegbahn et al., 2019).

The d orbitals in Ni are relatively close in energy, which allows redistribution of electrons and accommodates a variety of ligands in different coordination geometries (Alfano and Cavazza, 2020; Siegbahn et al., 2019). Ni(II) exhibits flexibility in adopting coordination numbers typically between four and six, often forming square-planar or octahedral complexes depending on the ligand field. By contrast, Fe, with its larger number of unpaired 3d electrons, tends to adopt specific coordination geometries such as octahedral or tetrahedral to minimize electron repulsion (Liu et al., 2024). The type of ligands and the local chemical environment further influence the coordination geometry and reactivity of Ni complexes in biological systems (Alfano and Cavazza, 2020; Siegbahn et al., 2019).

2.3. Oceanic nickel

Dissolved Ni in oceanic environments exhibits a nutrient-like vertical distribution, with depleted concentrations in surface waters and increasing concentrations with depth (Sclater et al. 1976). This pattern is reinforced by correlations between Ni and phosphate in surface waters, and between Ni and silica in deeper waters (Bruland 1980).

In the upper water column, a positive correlation between Ni, nitrate and phosphate reflects Ni's involvement in biogeochemical cycling. Similar to phosphate and nitrate, Ni is assimilated by phytoplankton, cyanobacteria and diatoms near the surface, where biological uptake depletes these elements in shallow waters (Price & Morel 1991; Dupont et al. 2008a,b). As organic material containing Ni, nitrate and phosphate sinks and decomposes, these elements are released at subsurface levels, creating maxima at depth. Nickel's association with organic material is due to its roles in various metabolic functions, including key enzymatic processes related to nitrogen and carbon cycling. Under surface oxidative conditions, Ni is stabilized as the divalent ion Ni^{2+}, allowing it to be bioavailable for these biological processes. Thus, Ni depletion in surface waters reflects high biological activity, where nitrate, phosphate and Ni are utilized by organisms.

In deeper waters, Ni concentrations correlate more strongly with silica, showing a deep maximum aligned with peaks in silica from diatom dissolution (Bruland 1980). Diatoms, which incorporate silica into their frustules, eventually sink and decompose at depth, releasing both silica and Ni. Unlike phosphate, which is more readily recycled in surface waters, silica accumulates primarily in deep waters. This suggests that Ni regeneration is linked to silica through the decomposition of silica-bearing organisms.

Redox chemistry also plays a key role in Ni distribution at depth. In less-oxygenated regions, redox changes facilitate Ni release from decomposing organic-rich particles, further aligning Ni regeneration with nitrate, phosphate and silica cycles. Low oxygen levels can enhance the association of Ni with organic particles, releasing it during remineralization. Nickel adsorption onto Fe-Mn oxides is common in oxic conditions; however, in deeper, reduced environments, Fe and Mn oxides may dissolve, releasing adsorbed Ni back into the water column.

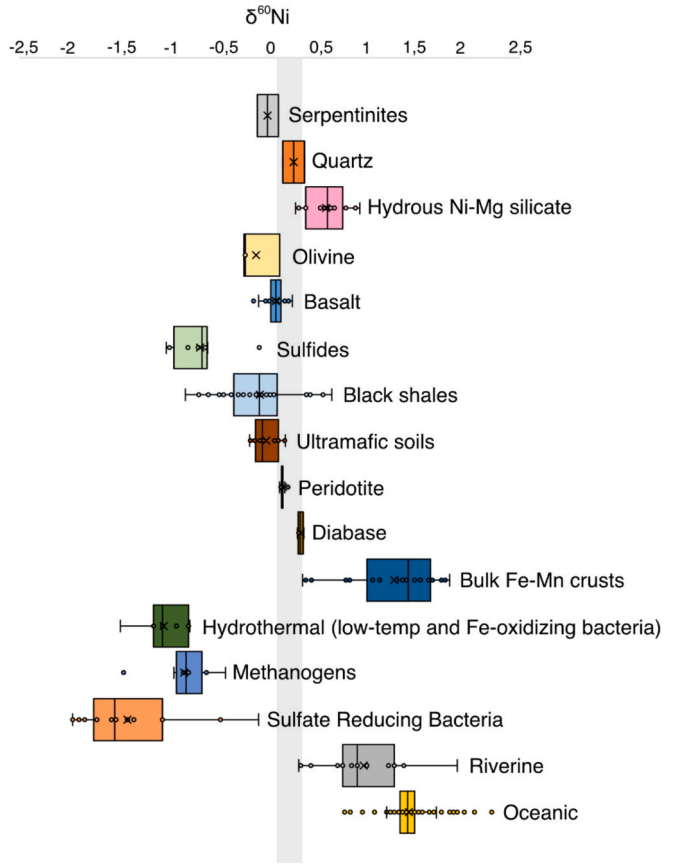

Fig. 2. Box plot showing Ni isotope composition in ‰ of various natural and laboratory samples from the literature (Spivak-Birndorf et al., 2018, Gall et al 2012, 2013, Gleeson 2004, Gueguen et al., 2013, 2021, Ratie et al. 2015, Ratnayake et al. 2021, Wang et al. 2021, Klaver et al. 2020, Li et al. 2020, Beunon et al. 2020, Wu et al. 2019, Chernonozhkin et al. 2015, Steele et al. 2011, Chen et al. 2023, Cameron et al. 2009, Cameron and Vance, 2014, Lemaitre et al. 2022, Archer et al. 2020, Sorensen et al. 2020, Pašava et al. 2016, Hein et al, 2013). The gray area represents the BSE $\delta^{60/58}$Ni value modified from Hiebert et al. 2020).

This dynamic uptake and release of Ni, via biological processes in the upper waters and from particulate matter under reduced conditions at depth, contributes to its deep maxima and its association with silica.

In oceanic regions, total dissolved Ni in the euphotic zone typically stays above 1.5–2 nM, posing a challenge to the theory of Ni–N co-limitation unless a substantial portion of Ni is unavailable in bioactive forms. Like many metals, Ni often forms complexes with organic ligands, reducing its bioavailability; estimates suggest 25% to 99.9% of Ni is organically bound (Cameron and Vance, 2014). Nickel has a residence time in the ocean estimated at 4–10 kyr (Gall et al., 2013; Sclater 1976), with rivers contributing the largest input (Cameron and Vance, 2014), and smaller sources from dust and hydrothermal fluids. Its primary removal mechanism is through scavenging by Fe–Mn oxides. Unlike some other metals, Ni concentrations are not strongly influenced by low-oxygen or euxinic conditions, as observed in the Black Sea where Ni is only slightly enriched. However, Ni is significantly enriched in non-sulphidic, upwelling areas, such as the Peru Margin, which suggests organic matter export as an important sedimentary sink for Ni.

2.4. Nickel isotopes

Ni stable isotope data is expressed as δ^{60}Ni, which is the per mil deviation of Ni^{60}/Ni^{58} ratios relative to the standard NIST SRM 986. The first publication proposing the potential utilization of Ni isotopes as a biosignature dates back to 2009, when pronounced accumulation of light Ni ($\Delta^{60}Ni_{cells\text{-}starting\ medium}$ as large as -1.41 ‰), in contrast to meteorites or basalts (+0.27 and +0.15 ‰, respectively), was shown based in laboratory experiments with methanogens (Cameron et al. 2009) who highly depend on Ni (Fig. 2). Notably, other archaea (*Pyrobaculum calidifontis*) demonstrated a lesser affinity for light Ni accumulation ($\Delta^{60}Ni_{cells\text{-}starting\ medium}$=+0.11‰), implying the plausible use of Ni isotopes as a class specific indicator. Nevertheless, laboratory experiments with sulfate reducing bacteria have shown a similar strong fractionation effect as with the methanogens, and where the total fractionation between the growth medium and the solid Ni sulfides were as large as -1.99‰ (Parigi et al., 2022). Subsequent laboratory investigations, however, have demonstrated that both Fe oxides (Wang and Wasylenki, 2017, Neubeck and Freund, 2020, Wasylenki et al. 2015) and Mn oxides (Sorensen et al. 2020) accumulate light Ni (~0.4‰ and as large as -3.35‰, respectively), thereby complicating the viability of Ni-isotopes as a definitive biosignature, given the prevalence of these minerals in the geological rock record. Limited studies have successfully identified a biogenic Ni isotope signature in natural soils (Ratié et al., 2019) but the biogenic influence on Ni isotopes is evident in the massive Fe oxyhydroxide deposits at ~5000 mbsf near the hydrothermal field of Lōihi Seamount (Hawaii), where the Fe and Mn-rich deposits show a considerable lighter isotopic composition of -1.06‰ (Gueguen et al., 2021; Edwards et al., 2011). This is in contrast with hydrogenetic Fe-Mn nodules that range from +0.9‰ to +2.5‰ or bulk oceanic (Gueguen et al., 2021). The hydrogenetic Fe-Mn crusts are lighter in the Pacific (+0.37‰) than in the Atlantic Ocean (+1.05‰). Oceanic, Mn-rich, oceanic sediments have δ^{60}Ni values around +0.26‰, whereas carbon-rich suboxic sediments show lighter values of -0.08‰ (Fleischmann et al., 2023).

The importance of Ni for biology is also visible in key enzymes in prokaryotic and eukaryotic organisms (Ragsdale, 2007, 2009) or in depth profiles of the seawater column, where Ni follows a nutrient-like distribution (Sclater et al. 1976; Bruland 1980; Mackey et al. 2002). The first Ni isotope analyses of seawater showed heavier isotopic values at greater depths (+1.4‰), in concordance with other trace metal isotope values (Vance et al., 2008; Cameron and Vance, 2014; Takano et al. 2017; Wang et al. 2019a) and lighter values at the surface waters (+1.7‰). The main source of Ni to the oceans are riverine, continental crust weathering sources, dust, aerosols and hydrothermal vent fluids (Wang and Wasylenki, 2017; Gall et al., 2013; Cameron and Vance, 2014; Spivak-Birndorf et al., 2018). However, there is a mass balance problem in the global Ni budget, where the ocean is isotopically heavier (+1.4‰) than the collective sources (+0.8 ‰) and sinks (Gueguen et al., 2016, 2021; Gall et al., 2013). The primary output (sorption onto Fe–Mn oxides), exhibits a comparable isotopic composition to the dissolved phase (+0.9 to +2.4‰), whereas the input from rivers, (+0.80‰, Cameron and Vance, 2014) is relatively lighter than the dissolved marine pool (+1.44 ± 0.15‰, Cameron and Vance, 2014; Gueguen et al., 2016, 2021; Gall et al., 2013; Vance et al., 2016). Several studies have thereafter been performed in order to close this mass imbalance, by mapping the average continental crust (Ratié et al., 2019; Klaver et al. 2020; Machado et al., 2023), euxinic sediments (+0.3‰) and black shales (-1 to +2.5‰). In the Black Sea, Ni concentrations in euxinic sediments are enriched despite similar levels in surface and deep waters (Vance et al., 2016). This phenomenon can be explained by a benthic Fe/Mn redox shuttle that transports Ni from the shelf to the open basin via nano-particulate oxides. A fine particle layer enriched in Mn and trace metals, including Ni, forms through the reoxidation of sediment-derived reduced Mn and Fe. The isotope composition indicates that the overall input of Ni is lighter (~+1.0 to 1.3‰) than the water (~+1.35‰). The isotope compositions thus suggest that Ni inputs to the sediments, after fractionation into sulfidized species (~+0.7‰, Fuji et al. 2014), are consistent with observed values, indicating a complex interplay of sources and sinks.

The Ni isotopic composition of terrestrial rocks ranges from -1,04‰

to +2.5‰ (Spivak-Birndorf et al., 2018; Cameron, 2009; Gueguen et al., 2013; Gall et al., 2013; Ratié et al., 2019; Estrade et al. 2015; Cameron and Vance, 2014; Porter et al. 2014; Vance et al., 2016). The lightest δ^{60}Ni values are typically associated with sulfide-mineralized ultramafic magmas (komatiites) and black shales (-1,04 and -0,84‰, respectively), while the heaviest values are found in hydrous Ni-Mg silicates (Pašava et al. 2019; Gall et al., 2012, Gall et al., 2013; Ratié et al., 2019; Spivak-Birndorf et al., 2018). Ultramafic magmas rich in sulfide minerals display highly negative δ^{60}Ni values with significant variability, likely resulting from magmatic processes such as sulfide liquid segregation from komatiitic lavas and subsequent fractional crystallization (Hiebert et al., 2022). Similarly, large δ^{60}Ni variations are observed in continental flood basalts from the Noril'sk region in the Siberian Trap large igneous province. These variations have been attributed to the immiscibility of sulfide-silicate magmas, leading to the preferential association of light Ni isotopes with the sulfidic phase (Chen et al., 2009). Weathering of rocks is associated with relatively large variations of δ^{60}Ni, where light Ni is preferentially incorporated into the solid precipitates, clays or oxides whereas the fluids are enriched in the heavy Ni isotope (Ratié et al., 2019, Wasylenki et al. 2015, Spivak-Birndorf et al., 2018, Neubeck and Freund, 2020) (Fig. 2).

2.5. Serpentinization

Serpentinization is an exothermic, alteration process occurring in ultramafic rocks under hydrous conditions, wherein the ferromagnesian minerals, notably olivine or pyroxene, react with aqueous fluids, yielding a suite of secondary minerals dominated by serpentine. The serpentinization reaction involve the hydration of olivine (or pyroxene) into serpentine minerals. Sometimes, at low silica activity (Frost & Beard, 2007) and strongly reducing conditions, $H_{2(gas)}$ can be formed as a byproduct through the splitting of water according to equation 1 below.

Since Fe and Ni ions are released into the solution as part of the alteration process, H_2 may further reduce both to native metals or their alloys such as Ni_3Fe (awaruite, one of the most widespread Ni–Fe alloys found in hydrothermal vents) within the serpentine system (Dekov, 2006, Pernet-Fischer et al. 2017, Sleep et al., 2004, Britten, 2017, Mével, 2003, Klein and Bach, 2009, Plümperet al. 2017). Not only is the formation of H_2 of great importance for the onset and maintenance of life as an electron donor for the most ancient and the only energy-releasing route of biological CO_2 fixation, the reductive acetyl-CoA pathway, it may also act as a reducing power for the abiotic formation of reduced carbon species such as CH_4, an important carbon source for microbial life (Horita & Berndt 1999, Preiner et al., 2018, Lamadrid 2017, Holm et al., 2015). The C=O double bond in CO_2 has a relatively high dissociation energy (749 kJ/mol) and need to be cleaved in order to further react into organic compounds. The cleavage in question has been extensively reported to proceed on FeNi catalysts (Hudson et al., 2020; Lv et al. 2016; Varma et al., 2018; Preiner et al., 2020; Beyazay et al. 2023), where Fe and Ni fulfill distinct catalytic functions. Iron exhibits a stronger affinity for oxygen species, whereas Ni facilitates carbon activation (Moret et al., 2014). Furthermore, a charge transfer from Fe to Ni has been proposed, potentially increasing the electron density at the Ni site and thereby enhancing its catalytic activity relative to that of a pure Ni^0 catalyst (Beyazay et al. 2023; Yadav and Kharkara, 1995). In a serpentinizing system, awaruite and/or Ni^0 has the capacity to both split water and to catalyze the formation of formate, acetate and puryvate from CO_2 (Beyazay et al. 2023, Jeoung et al. 2007). Further, in studies by Preiner et al. (2020), awaruite was tested for its capacity to convert CO_2 into acetate (common substrate for methanogens) at relatively low temperature (100°C) hydrothermal conditions with pH > 8, as an analogue to serpentinization environments and the results clearly showed a thermodynamically favourable (ΔG= -132 kJ/mol) formation of acetate. This is of interest because it demonstrates that serpentinization at relatively low temperatures can generate organic nutrients for microorganisms in an abiotic setting, such as the Lost City Hydrothermal Field, which is suggested to be driven entirely by serpentinization (Ludwig et al., 2011).

Hotter hydrothermal vents such as black smoker type vents, with temperatures between 200°C and 400°C, are driven primarily by proximity to a magma chamber and not serpentinization (Kelley et al., 2001, 2005). Some serpentinization-hosted vents, however, are characterized by acidic pH values, high H_2 and metal concentrations and generation of smaller hydrocarbons (C1-C5). At the vent chimney walls, consisting of precipitated sulfides (commonly FeS), the water-mineral interface can act as an electrocatalyst capable of catalytically reducing CO_2 in slightly acidic pH regimes (Nakamura, et al. 2010). In another study by Yamaguchi et al. (2014) it was experimentally shown that electric currents flowing through the hydrothermal chimney walls (as an electrical gradient) through the interconnected micron- and submicron-crystalline particles of FeS, inefficiently converted CO_2 into hydrocarbons. However, with the substitution of Fe with Ni, the electrosynthesis of organic compounds increased drastically and the electrochemical gradient across the chimney wall was maintained by a constant generation of electrons through the oxidation of H_2. These electrons are stored in the inner mineral precipitates via the dissociative insertion of H_2. These findings shed light on how hydrothermal vent deposits conduct electrons and catalyze reactions, and their potential for storing energy to drive the synthesis of organic compounds before the emergence of early life forms. In a similar manner, this redox gradient can be found within a euxinic sediment (Algar et al., 2020). The pH gradients in a euxinic sediment may be large due to microbial sulfide oxidation and the concomitant formation of electrical currents, in so-called sediment microbial fuel cells (SMFCs). Also, the Fe^{2+}/Fe^{3+} redox couple may aid in the formation of a redox and/or pH gradient through the interconversion of ferrous ions and ferric ions in pore waters. Under reducing conditions, such as those found in anoxic sediment layers, electrons released during Fe^{2+} oxidation can participate in redox reactions and may contribute indirectly to H_2 formation in the presence of catalytic minerals. During the oxidation of ferrous ions, electrons are released and can reduce water into H_2 gas. This reaction may be further facilitated by heterogeneous catalysts such as a Ni containing Fe sulfide, which is precipitated within the euxinic sediment column (Mansor et al. 2019).

Given that hydrothermal vents have existed on Earth for billions of years and considering that the emergence of life presumably requires a significant amount of time, this fulfills a critical criterion for the initiation of life: namely, that sufficient time has elapsed for life to begin. Although individual hydrothermal vents have limited lifespans, ranging from several years to a maximum of around 100,000 years (Früh-Green et al., 2003; Ludwig et al., 2011), prebiotic systems could have been transported between neighboring vents, allowing continuity for chemical evolution.

2.6. Black shales

Black shales are one of the most important geological records for early signatures of life. They are dark-colored, fine-grained and organic and S rich sedimentary deposits that have been formed on earth for at least 3.2 billion years (Van Kranendonk, 2008; Jin et al. 2023). They form under oxygen depleted or anoxic conditions with incomplete degradation of organic matter, leading to excellent preservation conditions for ancient life but also of other geological events. Black shales commonly consist of four main components; organic matter, sulfides, siliciclasts and carbonates, where siliciclasts make up the major part of the rock (Oschmann 2011; Röhl et al. 2001). The sulfides and organic matter within a black shale is mainly thought to be derived from bacterial Fe- and sulfate reduction, but studies have shown that also methanogens (Payne et al. 2023) as well as methane oxidizing archaea (Schouten et al. 2001) inhabit euxinic or ferruginous environments. Methanogens in euxinic environment are able to to reduce pyrites into available Fe^{2+} and HS^- and approximately 5-8% of the total

methanogenic encoded proteins are expected to bind [Fe-S] clusters (Johnson et al. 2021). There is a higher reliance on [Fe-S] clusters in methanogen cells compared to other facultatively anaerobic or aerobic cells which may stem from the high bioavailability of Fe, S and other reduced metals, namely Ni under anoxic/euxinic conditions (Liu et al. 2012) of the early Earth, where these organisms are believed to have diversified over 3.51 billion years ago. Euxinic environments are commonly rich in trace metals that reacts with the sulfides to form precipitates with limited solubility, but methanogens have been shown to catalyze the reductive dissolution of pyrite and nickelian pyrite (Payne et al. 2021, Spietz et al. 2023, respectively). Also, the availability of Ni^{2+} ions may be relatively high within euxinic environments, despite the lower solubility of Ni compared to other trace metal sulfides, leading to increased displacement of Ni into solution, making it more bioavailable (Zanella 2011). The solubility product of NiS is low (K_{sp}= 4.0 10^{-20} at 25°C) and may thus decrease the bioavailability of Ni in euxinic, sulfide -rich environments. Despite the challenges posed by sulfide, certain organic ligands and complexes can enhance the bioavailability of Ni under euxinic conditions, such as cysteine (Cys), glutathione, histidine-rich peptides as well as humic and fulvic acids. These ligands are all relatively stable under euxinic conditions and may have maintained sufficient bioavailability of Ni in sulfide-rich environments. Ni(II) forms stable binary and ternary complexes with adenine and L-amino acids, with Ni(II):Ade:L-Asn identified as the most stable (Türke, 2015). Such ligands may arise through abiotic synthesis or organic matter degradation, possibly catalyzed by mineral surfaces. These factors collectively suggest that such ligands played a significant role in making Ni and other metals bioavailable under early Earth conditions.

Nickel have been shown to follow the distribution of Mo in anoxic to oxic sediments, where the distribution decreases with increasing degree of oxidation (Zanin et al. 2017). Nickel and molybdenum are both transition metals, but they exhibit differences in solubility and oxidation state in natural systems due to their electronic configurations and chemical properties. Nickel typically exists in the oxidation state +2 in natural environments forming Ni sulfides (such as Ni monosulfide, NiS, Zanella 2011) or is incorporated into pyrites (Wu et al. 2023). Nickel sulfide solubility is more dependent on the choice of ligands than on the oxidation state. In contrast to Ni, molybdenum (Mo) is found in several oxidation states in nature, especially +2, +4, and +6. The oxidation state +6 is most common and are often found in oxyanions, such as MoO_4^{2-}, which are highly soluble in water. However, under anoxic conditions, Mo can undergo complex transition between different oxidation states, including +6, +4, and +2. Molybdenum(IV) and molybdenum (VI) species are more common, with molybdate (MoO_4^{2}) being the predominant form under aerobic conditions. Molybdenum sulfides, especially molybdenite, are often insoluble or mildly soluble under anoxic conditions and do precipitate. Thus, even though Ni and Mo follow each other in terms of environmental concentrations with shifting redox conditions, the underlying processes are different. Noteworthy, it is not entirely known of how Ni exactly travels through the environments. Molecular factors that influence the mobility of Ni and Ni-compounds are bond lengths (Liu et al. 2018), redox conditions and ligand complex binding (Zanella, 2011). Additionally, the amount of organic C and pyrite (Zanin et al. 2017), weathering (Ratié et al., 2019) and magmatic processes (Hiebert et al. 2022), are essential, just to mention a few factors. Despite these ambiguities, Ni is often strongly enriched in black shale deposits which constitute ideal environments for the preservation of Ni signatures (concentrations and isotopes) and biosignatures but also for large scale geological events such as greenhouse climates, periods of enhanced global volcanism, continental flooding and anoxia events.

The Ni isotopic composition of black shales varies considerably between ~-1 to~+2.5‰, depending on the formation and deposition conditions of the black shales (Porter et al. 2014, Li et al., 2021, Pašava et al. 2019.). According to Porter et al. (2014), no correlation between total organic carbon and stable Ni isotopes could be detected, which was later confirmed by Pašava et al (2019).

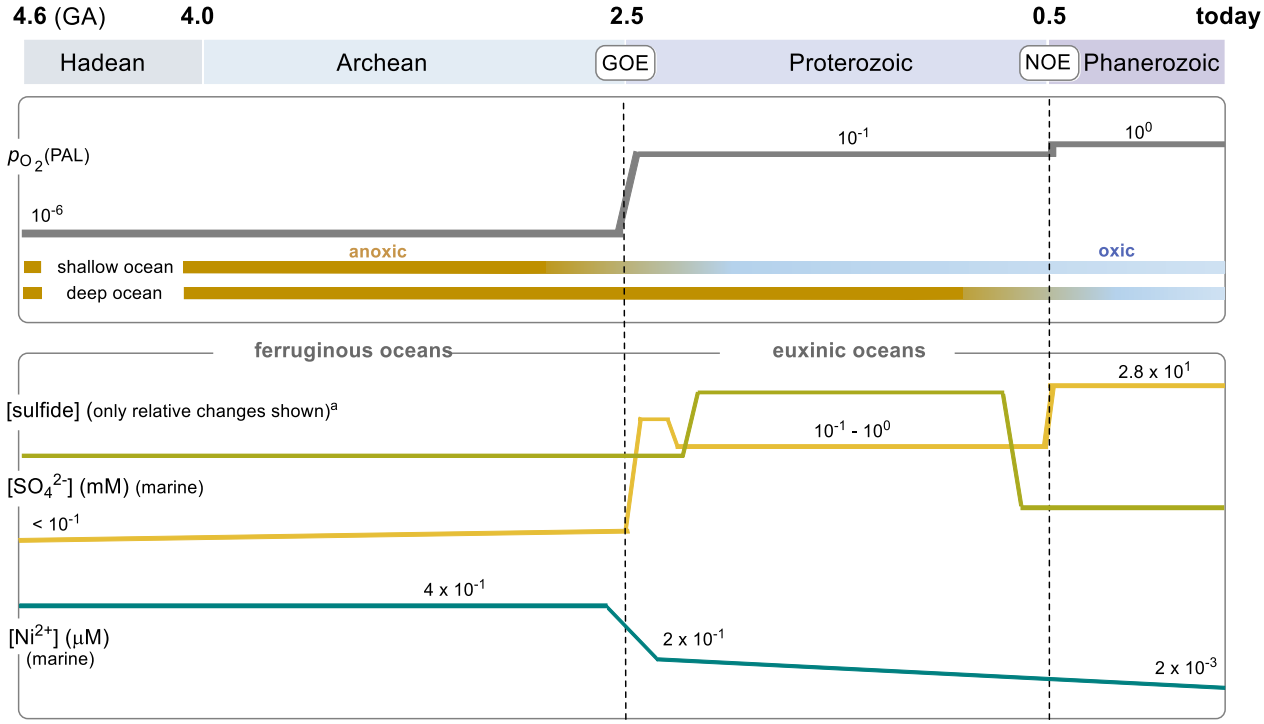

Fig. 3. Simplified geological history of atmospheric oxygen and oceanic redox states including that of relevant S and Ni species (S species: Olson and Straub, 2008; Ni: Konhauser et al., 2009, 2015); pO_2= atmospheric partial pressure of O_2; PAL= present atmospheric level) (Fakhraee et al., 2019). The concentrations indicated by the lines are not scaled but give a semi-quantitative impression. In particuar sulfide concentrations are under debate (Lyon 2008 and Fakhraee et al., 2024).

2.7. Mass extinctions

2.7.1. Great oxygen event (GOE)

One of the most dramatic extinction events on Earth is attributed to the fundamental change that made the planet habitable for today's life forms, namely the dramatic increase in atmospheric oxygen. It marks the transition from the Archaean to the Proterozoic. This event is called the Great Oxygenation Event (GOE) and evidenced several concomitantly occurring dramatic shifts in Earth surface environments, such as the increase in atmospheric O_2 and a shift towards a more felsic crustal composition (Keller & Schoene, 2012), increased subareal volcanism (Kump & Barley, 2007), drop in atmospheric methane (Catling et al. 2001), increased weathering of felsic continental crust leading to a plunge in marine transition metal concentration (Wang et al. 2019; Konhauser et al., 2009; Konhauser et al., 2015) and increased weathering of sulfides (Wang et al. 2019) (Fig. 3). The suggested reason for this Ni decline is the secular cooling of the mantle and the followed decline in high-temperature lavas such as komatiites, which have been suggested to be one of the main Ni sources during the Archean (Liu et al. 2021; Hall, 1987).

The marine Ni concentrations declined from ~400nM at 2.7 Ga to ~200nM approximately 200 Ma later, which have been proposed as a major cause for the decline in methanogenic activity (and the concomitant decline in atmospheric methane), paving the way for oxygenic microorganisms such as cyanobacteria. With an increasing concentration of atmospheric oxygen comes the increased oxidation of reduced minerals such as the abundant sulfides into sulfates, which accumulated in the oceans. Increasing sulfate concentrations in marine environments, will concomitantly benefit sulfate reducing bacteria and a secular increase in shallow euxinic conditions. In turn, euxinic conditions and environments rich in sulfides will readily bind Ni and form insoluble Ni bearing Fe sulfides and pure Ni sulfides, such as pyrites, pyrrhotites, millerites and pentlandites. It has been shown that methanogens can use solid Ni sulfide minerals as a Ni source (Spietz et al. 2023).

[a] Current H_2S concentration in the Baltic sea in relation to sea depth: 0 μM @ 70 m, 9 μM @ 100 m and 16 μM @ 150 m (Bauer et al., 2017).

The decline in atmospheric methane may have resulted from increased competition between methanogens and sulfate reducers for ecological niches. An alternative hypothesis associates the Great Oxidation Event (GOE) with a decline in bioavailable Ni, inferred from the decreasing Ni/Fe ratios in banded Fe formations dated to around 2.7 Ga. This trend is thought to result from diminished Ni contributions linked to the waning eruption of ultramafic rocks as the mantle cooled. Given methanogens' reliance on Ni-containing enzymes—especially MCR, which constitutes ~10% of their cytoplasmic proteins—a Ni shortage could have led to their decline, allowing sulfate reducers and oxygenic phototrophs to thrive. Nickel isotopes help clarify the relationship between Ni availability, methanogens, and the GOE. The notion that Ni flux to the oceans dropped as a consequence of the weathering of new, low-Ni upper continental crust (UCC) has been disputed by Wang et al. (2019) based on stable Ni isotope data. In their study, glacial Precambrian diamictites covering the GOE were analyzed. The geochemical weathering signatures preserved in the diamictites are interpreted as reflecting contributions from the upper continental crust (UCC), offering a more representative snapshot of the crustal composition during their deposition. A progressive enrichment in heavier δ^{60}Ni values, accompanied by a decline in Ni concentrations, is observed in these sediments approaching the time of GOE, suggesting a long-term shift in crustal Ni cycling.The suggested cause for this rise in δ^{60}Ni was the onset of oxygenic weathering of crustal sulfides, leaving the diamictites lower in light Ni and lower in total S and Ni concentrations. Not only are sulfides the only major Ni containing rocks types that have distinct different isotopic values from silicates (Gueguen et al., 2013; Hofmann et al. 2014; Gall et al. 2016; Cameron et al. 2009; Chernonozhkin et al. 2015), sulfides are more strongly binding ligands for Ni than halides, hydroxide, sulfate, carbonate and carboxylates making them more stable during the anoxic conditions prevailing before the GOE. This makes Ni isotopes a suitable tool for targeting changed sulfide weathering patterns across time. Determining the dominant hypothesis in this field remains challenging, but it is evident that a decline in bioavailable Ni would have severely impacted methanogen populations. These archaea rely on Ni for essential enzymatic functions, particularly in methane production. Even today, Ni scarcity can limit methanogenic activity, highlighting the metal's crucial role in their metabolism.

2.7.2. End-Perm

The end-Permian mass extinction (EPME), one of the largest in Earth's history, occurred at the close of the Permian period. It is associated with the eruption of enormous amounts of basaltic magma, which formed the Siberian Traps Large Igneous Province (STLIP) (Hall, 1996). This massive continental flood basalt event is believed to have contributed to the extinction, which resulted in the loss of approximately 90% of marine species and 75% of terrestrial species. The EPME marks a catastrophic disruption in the carbon cycle, evidenced by carbon isotopes (Holser et al., 1989), charcoal-rich sediment, widespread anoxia and euxinic sediment layers (Shen et al., 2011). As for the transition from an anoxic to an aerobic world during the GOE, the EPME was also suggested to be triggered by Ni concentrations and methanogenesis. (Rothman et al., 2014). Prior to the EPME, there was an enormous rise in Ni concentrations in the atmosphere and oceans due to the emplacements of NiS ore-bearing intrusions in the STLIP (Le vaillant et al. 2017). The remarkable event of releasing Ni (for which no volatile Ni containing derivatives are known) into the atmosphere, resulting in a much broader spatial dispersal, has been modeled by Le Valliant et al. (2017). They demonstrated that the flotation of Ni sulfide liquid droplets, facilitated by attachment to gas bubbles, and the degassing of volatile sulfide-saturated volcanic gas led to a global dispersal of Ni. As Ni concentrations increased, the two-step acetate kinase (AckA)-phosphoacetyl transferase (Pta) pathway emerged, alongside the acetoclastic methanogen *Methanosarcina* (Rothman et al., 2014; Fournier and Gogarten). This pathway marked a significant development in methanogenesis. It has been suggested that the Late Permian environments of low marine O_2 and sulfate would be beneficial for extensive growth of *Methanosarcina*, leading to an explosive increase in atmospheric CH_4 and enhanced anoxicity. Since *Methanosarcina* are cytochrome-bearing methanogens, the growth yield (and thus CH_4 formation) is much larger than the capacity of non-cytochrome-bearing methanogens for CH_4 formation. Thus, it is feasible to assume that explosive growth of *Methanosarcina* may have occurred. Additionally, *Methanosarcina* requires much more Ni for their growth, which may have been beneficial during the Late Permian with high Ni availability. However, the sensitivity of *Methanosarcina* to available Ni also makes them vulnerable to Ni decline, likely marking the end of the EPME. Nickel isotope analyses have been conducted on the black shales of the Siberian Traps (Li et al., 2021) to investigate the putative impact of Ni on the mass extinction since both an increase in methanogenesis and increased diagenesis have been proposed as triggers (Froelich et al 1979). Nickel isotopes have been previously shown to be strongly fractionated by methanogens under laboratory conditions (Cameron et al. 2009), where the preferentially accumulate the lighter isotope, leaving the growth medium isotopically heavy. The Ni isotopic signature prior to EPME showed extremely light values, ranging from -0.89 to -1.09‰ and increases to approximately 0.34‰ at the extinction horizon, where the Ni concentration sharply drops from 142.8 to 36.4 ppm. This suggests that the increase in available Ni not only enhanced methanogenesis, potentially contributing to global anoxic events and associated mass extinctions, but also that the natural stable Ni isotope signatures are consistent with laboratory experiments demonstrating the significant isotopic fractionation imparted by methanogenic activity.

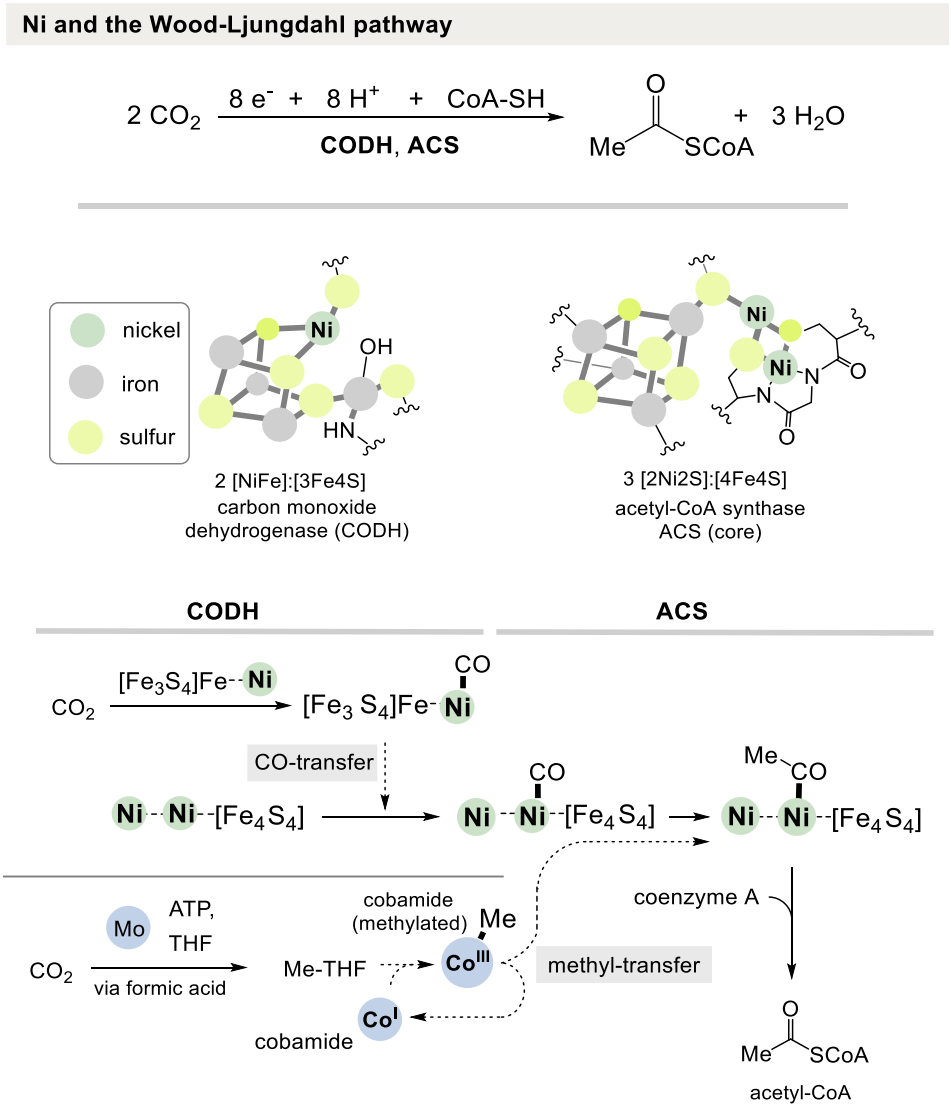

Fig. 4. The role of Ni in C1 fixation: The reductive acetyl-CoA pathway (Wood-Ljungdahl pathway) relies on Ni- Fe-S clusters and on molybdenum and cobalt cofactors.

3. Nickel biochemistry

3.1. Ni in metabolic pathways

3.1.1. CO_2 fixation, the Wood-Ljungdahl (WL) pathway and prebiotic analogs

The Wood–Ljungdahl (WL) pathway represents a non-cyclic route of autotrophic carbon fixation, in which carbon dioxide is sequentially reduced and condensed to yield acetyl-CoA. This process is catalyzed by a tightly coupled enzyme complex composed of carbon monoxide dehydrogenase (CODH) and acetyl-CoA synthase (ACS). These enzymes are rich in redox-active centers, notably [4Fe–4S] clusters and Ni-Fe catalytic sites. In CODH, a specialized [Ni–4Fe–4S] cluster mediates the reduction of CO_2 to CO. The resulting CO is channeled to ACS, where it combines with a methyl group—supplied by a cobalt-containing corrinoid Fe-S protein (CoFeSP)—to form an acetyl intermediate at a bimetallic Ni site bridged to a [4Fe–4S] cluster. This intermediate is then converted into acetyl-CoA through thioester exchange with coenzyme A. Nickel incorporation is essential for CODH activation and is coordinated by accessory proteins such as CooC, CooT, and the histidine-rich CooJ, which binds Ni(II) at two distinct sites (Evans, 2005; Drennan, 2004; Ragsdale et al., 1985; Drennan et al., 2001).

Contemporary origin-of-life models often emphasize chemoautotrophic scenarios in which carbon dioxide served as the primary carbon source for early biosynthetic processes. Such carbon fixation must have emerged prior to the divergence of the Last Universal Common Ancestor (LUCA), the inferred progenitor of all cellular life. Among the proposed carbon fixation mechanisms, two stand out for their prebiotic plausibility: the reductive acetyl-CoA pathway (also known as the Wood–Ljungdahl, or WL, pathway, Ragsdale and Pierce, 2008; Ragsdale, 2008) and the reverse tricarboxylic acid (rTCA) cycle, including its simplified forms. This review places particular emphasis on the WL pathway due to its linear reaction sequence, which culminates in the formation of acetyl-CoA—a metabolite of central biochemical relevance (see Fig. 4). Transition metals, especially Ni, play a key catalytic role in this pathway, alongside Fe, cobalt, and molybdenum. The WL pathway is often favored over the rTCA cycle in prebiotic contexts because of its linearity. This structural feature addresses a core concern articulated by Orgel (2008), who argued that low reaction yields in abiotic systems pose serious limitations for autocatalytic cycles, since each step is contingent upon the successful completion of the previous one. This casts doubt on the enthusiasm of chemists to mimic metabolic cycles such as the rTCA cycle with prebiotic chemistry. Secondly, a bioinformatic analysis by Martin and coworkers (Weiss et al., 2016)

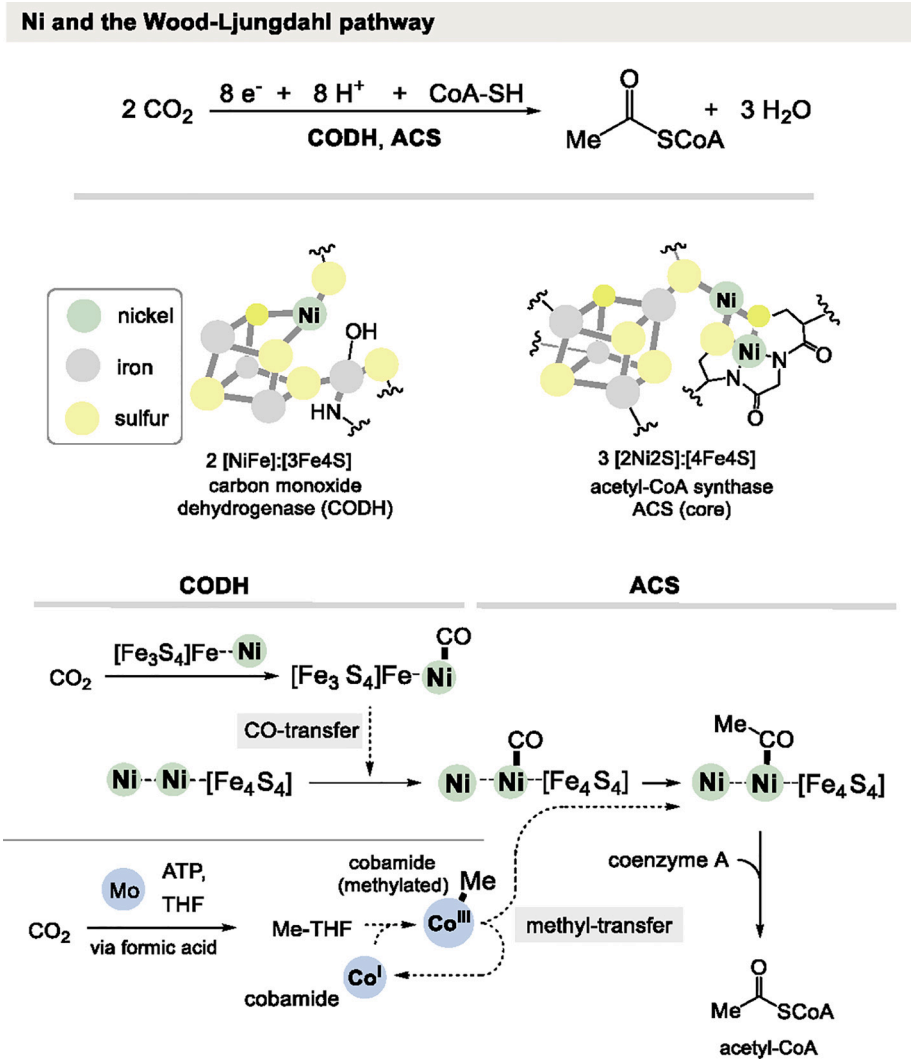

Fig. 5. Prebiotic chemistry mimicking the WL-pathway using Ni and attempts to mimick the *r*TCA cycle under prebiotic conditions.

suggests that LUCAś metabolism was based on the linear WL pathway. Other theoretical considerations on the evolutional role of coenzymes, in particular pyridoxal phosphate and thiamine pyrophosphate, do not support the idea that the rTCA cycle could have been the first metabolic system for C1 fixation (Kirschning, 2024). In line with these theories, contemporary organisms that utilize the WL pathway thrive in primordial environments abundant in inorganic gases like CO_2, H_2, and H_2S, as well as reduced metals such as Fe and Ni. The uniqueness of the WL pathway provoked to mimick it under plausible prebiotic conditions. The different experimental approaches commonly rely on Ni, in several cases acompanied by Fe. Pioneers in this field are Huber and Wächtershäuser, the latter being the first to formulate the so-called Fe-S

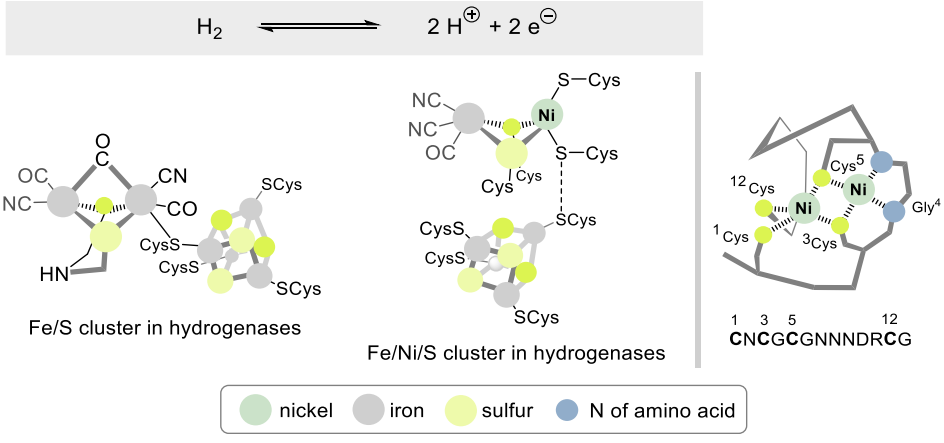

Fig. 6. Fe/S and Fe/Ni/S cluster in hydrogenases and a di-Ni hydrogenase model with a truncated peptide template.

hypothesis (or iron-sulfur world) on the origin of life (Wächtershäuser, 1988 & 1990). The hypothesis claims that Life on Earth originated on the surface of Fe-S minerals such as pyrite. Deposits of Fe sulfide minerals near deep-sea hydrothermal vents that originated of from reduced fluids (van Dover, 2009) are capable of providing the environment and energy to catalyze complex reaction sequences from simple precursors such as CO and CO_2, HCN and H_2S. They demonstratedthat methanethiol (CH_3-SH) and carbon oxysulfide (COS) are formed from CO_2 and FeS/H_2S, or from CO and H_2 in the presence of NiS (Fig. 5-I) (Heinen and Lauwers, 1996). The formation of several other S-containing organic molecules were detected in simulated laboratory experiments. Unusually high concentrations of carbon monoxide (350 mM), hydrogen sulfide, and methanethiol (8 mM) (Reeves et al., 2014) in the presence of Ni sulfide and Fe sulfide led to the formation of *S*-methyl ethanethioate (CH_3-CO-SCH_3), a simple analog of acetyl-CoA (Kitadai et al., 2021; Kitadai et al., 2024).

It was also demonstrated that natural Ni_3Fe (awaruite) is exceptionally efficient in aiding the abiotic synthesis of formate, acetate, pyruvate, and methane under mild (< 100 °C), hydrothermal conditions (Preiner et al., 2018; Martin, 2020) (Fig. 5-II). The carbonyl branch of the WL pathway is initiated by CO_2 reduction and formation of formate. Hudson and Sojo (Hudson & Soho, 2020) experimentally showed the reduction of CO_2 with H_2 at room temperature under moderate pressures (1.5 bar). The reduction supposedly is driven by microfluidic pH gradients across Fe(Ni)S precipitates and yielded formate. Deuterium labeling indicated that electron transfer to CO_2 does not occur via direct hydrogenation with H_2 but instead, freshly deposited Fe(Ni)S precipitates appear to facilitate electron transfer in an electrochemical-cell mechanism with two distinct half-reactions. Finally, Ni-Fe nitride (Ni_2Fe_2N) was shown to form formamide and formate from CO_2 and H_2O in the absence of hydrogen and nitrogen (Fig. 5-III). Here, water acts as hydrogen source and the nitride as nitrogen source (Beyazay et al., 2023b).

Although Orgel expressed skepticism regarding the feasibility of the reverse tricarboxylic acid (rTCA) cycle under prebiotic conditions, a number of experimental efforts have nonetheless sought to reconstruct this pathway using plausible early Earth chemistry. These studies frequently employ molecular hydrogen, elemental S, or sulfide compounds as electron donors or reductants. Notably, the group of Moran (Rauscher et al. 2022 and Muchowska et al., 2019) and others (Keller et al., 2017 and Kitadai et al. 2019) investigated the potential role of H_2 in driving a geochemically mediated analog of the rTCA cycle, proposing that such processes could have supported the assembly of primitive metabolic networks during the earliest stages of biochemical evolution. So far, it was demonstrated that three consecutive steps (oxaloacetate→malate→fumarate→succinate) of the reverse tricarboxylate (TCA) cycle, can be driven in one-pot by H_2 using fairly large catalytic amounts of a synthetic Ni source (10–20 mol%) (Fig. 5-IV). However, the next step in the cycle has to be regarded a key hurdle to provide α-ketoglutarate (Kirschning, 2022b; Schoenmakers et al., 2024). It remains to be seen whether the cycle can be closed under prebiotically plausible conditions, and even if this were the case, Orgel's critical doubts about prebiotic cycles would still have to be taken into account.

In this context, several studies on prebiotic chemistry have linked Ni as both a catalytic promoter and in hydrogen transfer chemistry with modern coenzymes. It has been found that nickel(II) can efficiently catalyze the transamination of amino acids and keto acids, thereby mimicking the coenzyme pyridoxal phosphate (PLP) (Mayer et al., 2021; Kaur et al., 2024). In the presence of PLP, an acceleration of this process was found (Dherbassy et al., 2023). Furthermore, it has been shown that nickel is capable of reducing nicotinamide (NAD^+→NADH) in the presence of H_2 (Pereira et al., 2022).

3.1.2. *H_2 fixation*

Hydrogenases are metalloenzymes that catalyze the reversible interconversion of protons and electrons with molecular hydrogen (H_2). These enzymes play essential roles in energy metabolism, particularly in anaerobic microorganisms such as sulfate-reducing bacteria of the genus *Desulfovibrio* (see Fig. 6). Among the most extensively studied classes are the [NiFe] and [FeFe] hydrogenases, distinguished by their characteristic metal cluster architectures. Both classes occur widely in bacterial species, while [NiFe] hydrogenases are also found in archaeal lineages. Interestingly, [FeFe] hydrogenases have been identified in select eukaryotic organisms as well (Lubitz et al., 2014; Vignais et al., 2007). These enzymes typically feature dinuclear metal centers, either Ni-Fe or Fe-Fe, associated with [4Fe–4S] clusters, which mediate electron transfer. A third group, known as [Fe]-only hydrogenases, possesses a mononuclear Fe center coordinated through a single cysteine residue. Hydrogenases are frequently implicated in reductive processes, including the regeneration of redox-active cofactors and coenzymes such as $NAD(P)^+$, ferricytochrome c_3, ferredoxins, coenzyme F_{420}, quinones, and tetrahydromethanopterins. Anaerobes that use hydrogenases live in sediments, hot springs hydrothermal vents and other environments. They are able to transfer electrons onto sulphate or nitrogen dioxide. The use of hydrogen as an electron donor coupled with the ability to synthesize organic matter, through the reductive assimilation of CO_2, characterize the hydrogen-oxidizing bacteria. Hydrogen is also produced in N_2-fixing organisms: at least one mol of H_2 is formed for every molecule of N_2 reduced. In such organisms hydrogenase functions to recapture the energy-rich reducing equivalents.

The active site of [NiFe]-hydrogenases in *E. coli* requires at least seven enzymes and cysteine plays a crucial role for cyanide formation and transfer (Cammack et al., 2001, Vignais & Colbeau 2004). Cyanide is generated by the action of HypE and HypF with carbamoylphosphate serving as starting point for thiocyanate bound to cysteine in HypE, which then serves as cyanide donor in a complex formed between the

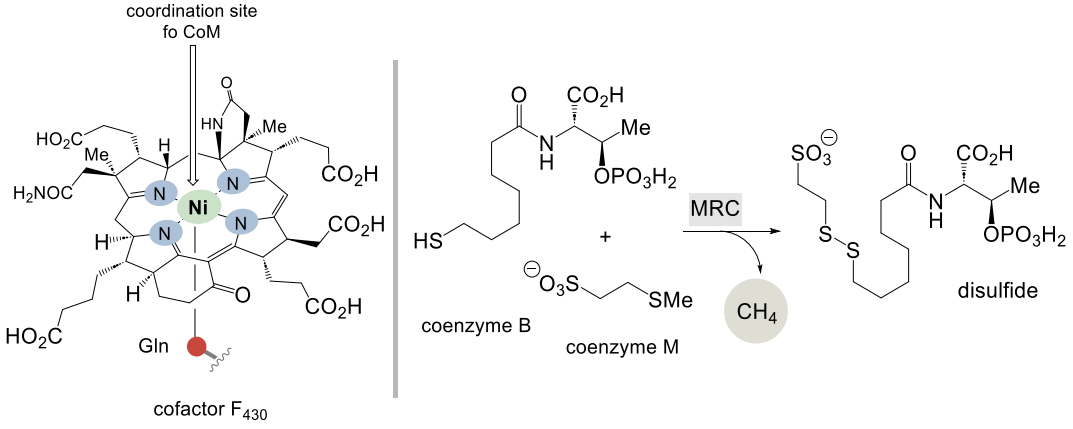

Fig. 7. Nickel-based cofactor F430 (left) and key step in methanogenesis (right) (Gln= glutamine).

maturation proteins HypC and HypD (Blokesch et al., 2004; Reissmann et al., 2003). The cyanide moiety on HypE is transferred to the Fe coordinating HypD/HypC complex, which is then transferred to the large subunit of the structural hydrogenase protein. The source of CO is unknown. The HypA and HypB proteins are responsible for delivering and incorporating Ni.

Recently, a simplified model of a hydrogenase composed of only 13 amino acid was reported (Timm et al., 2023) (Fig. 6, right). The peptide is able to bind two Ni ions. It was shown, that the di-Ni cluster formed is capable to produce molecular hydrogen from protons. Structurally it shows some analogy of a Ni-Fe cluster in [NiFe] hydrogenase and the Ni-Ni cluster. The authors suggest that despite their enormous complexity, hydrogenases are much older in that they evolved from simple peptide precursors. It is also worth mentioning that [NiFe]-hydrogenases are regarded to be more ancient from a phylogenetic perspective than [FeFe]-hydrogenases (Peters et al., 2015).

Hydrogenation catalysts are long known in the field of heterogeneous catalysis. Raney Ni is an old and famous example, an alloy that is mainly composed of aluminum and Ni which is able to activate hydrogen for hydrogenation of organic molecules. The same applies for the recently reported Ni silicide nanoparticle (Ryabchuk et al., 2018) and Ni catalysts that are composed of Ni/SiO_2 which are able to reduce CO to methane (Dias et al. 2021).

3.1.3. Methane formation

Less than 1% of all current methane is abiotically produced and a majority of the biogenic methane is formed by methanogens, with the help of the enzyme methyl-coenzyme M reductase (MCR). The MCR catalyzes the final step of the methane formation process, and methane formation is exclusively formed by archaea (Evans et al., 2019). It reductively forms a disulfide from methyl coenzyme M, a methyl thioether, with the thiol coenzyme B by which methane is liberated (Fig. 7). As a by-product the corresponding heterodisulfide is formed. Catalysis is promoted by the cofactor F_{430}, first discovered in *Methanobacterium thermoauto-trophicum*. It represents the most reduced tetrapyrrole present in the enzyme methyl coenzyme M reductase in methanogenesis (Thauer, 1998; Miyazaki et al., 2022). Theoretical and experimental data come to the conclusion of two principally different reaction mechanisms, one involving an organometallic methyl-Ni(III) species the second favouring a transient methyl radical species. The ligand sphere of the octahedral Ni environment is governed by the planar tetrapyrrole system with two axial sites that are occupied by Gln and during the biotransformation by coenzyme M.

In the context of this account the question of how Ni is chosen and incorporated into the sirohydrochlorin, the precursor of F_{430}, is of interest (Moore et al., 2017; Zheng et al., 2016), particularly in the context of its enzymatic insertion via CfbA. Proteins that are able to select metal cations such as Fe(II), Co(II) and Ni(II) for naturally occuring tetrapyrroles are called chelatases. Several of these enzymes are characterized by a histidine-rich region. In the present case, the class II chelatase CfbA catalyzes Ni^{2+} insertion and the ligand sphere of Ni is composed of two histidine (His) and one glutamate (Glu) residue and seems not to be linked with the histidine-rich region. CfbA is considered a significant ancestor of class II chelatases, acting not only as a Ni-chelatase but also as a cobalt-chelatase in vitro. Studies using X-ray crystallography indicate that the insertion of Ni^{2+} into sirohydrochlorin is facilitated by an acetate side chain within the ligand system (Fujishiro and Ogawa, 2021). These findings support the idea that the CfbA-mediated pathway in coenzyme F430 biosynthesis represents a crucial branching point, directing sirohydrochlorin toward the formation of both Ni- and Co-complexes. From an evolutionary point of view, the cofactor F_{430} is special because, despite its presumably ancient existence, the metal coordinates to nitrogen and is not bound to S like the other examples described so far. Biosynthetically, however, the four nitrogen atoms are recruited from the simplest and probably most abundant amino acid glycine in the abiotic and early biotic worlds (Kirschning, 2022b).

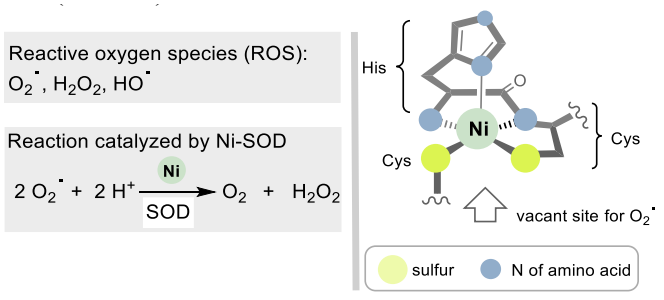

Fig. 8. Principal reaction that SOD catalyzes and ligand environment around Ni in Ni superoxide dismutase (Ni-SOD).

3.2. Nickel and O_2 handling

3.2.1. Ni-SOD

Superoxide is a byproduct of cellular respiration in aerobic organisms and can be the cause of severe damage to the cell (Pelmenschikov, 2006). The hexameric Ni superoxide dismutase (Ni-SOD) is a metalloenzyme that belongs to the superoxide dismutase family and serves as nature's defense mechanism towards superoxide. As such it catalyzes the disproportionation of the superoxide radical to H_2O_2 and O_2. Besides streptomyces it was also found in cyanobacteria and several other aquatic microbes (Zamble and Li, 2009).

The disproportionation mechanism involves a reduction-oxidation cycle where a single electron transfer is catalyzed by Ni, switching between Ni^{2+} and Ni^{3+} (Pelmenschikov, 2006; Shearer, 2014). The Ni complex is embedded in the protein being complexed by three histidine and two cysteine ligands (oxidized form shown in Fig. 8). One of the cystidines acts as a bidental ligand with the amide nitrogen atom also bound to the metal. Mechanistically, the proton source as well as the transfer mechanism are still being debated (Sheng et al., 2014). Interestingly, in the reduced form, the His ligand swings away, leaving a square-planar geometry.

The presence of ROS to early life, especially during the GOEmust have induced an enormous evolutionary challenge. Today, superoxide processing enzymes are widely distributed, both in the aerobic and the anaerobic living worlds and the Ni-SOD have the advantage of withstanding high ROS concentrations without damaging the enzyme, making it competitive in an aerobic world.

3.2.2. Acireductone

When molecular oxygen levels rapidly raised on earth about 2.5 billion years ago metalloenzymes with Ni as cofactor began to emerge that were able to deal with dioxygen and thus were able to promote oxidations instead of being involved in reductions. New ligand spheres and architectures appeared on the scene that were devoid of oxidation sensitive S or cysteine. One example is acireductone dioxygenase (ARD) that utilizes dioxygen as co-substrate. It is involved in the methionine salvage pathway (MSP) and either may contain Fe(II) or (Ni(II) as metal cofactor. The Fe complex utilizes 2-dihydroxy-3-keto-5-methylthiopent-1-ene (acireductone) as substrate which is oxidatively degraded by O_2 to 2-keto-4-methylthiobutyrate and formate. The Ni(II) isozyme uses the same substrate but promotes an off-pathway shunt to yield methylthiopropionate, carbon monoxide, and formate (Deshpande et al., 2017) (Fig. 9.I). It was found that not only Ni(II) but also divalent Mn(II) or Co (II) are able to promote this type of reaction. The two metal-dependent pathways catalyzed by ARD were initially identified in the bacterium *Klebsiella oxytoca*, but ARD enzymes have also been found in mammals, though not in archaea. In ARD, Ni is coordinated within a complex consisting of one glutamate and three histidine residues, while two positions in the octahedral environment, blocked by water, act as binding sites for the substrate acireductone. Nickel(II) is not directly involved in

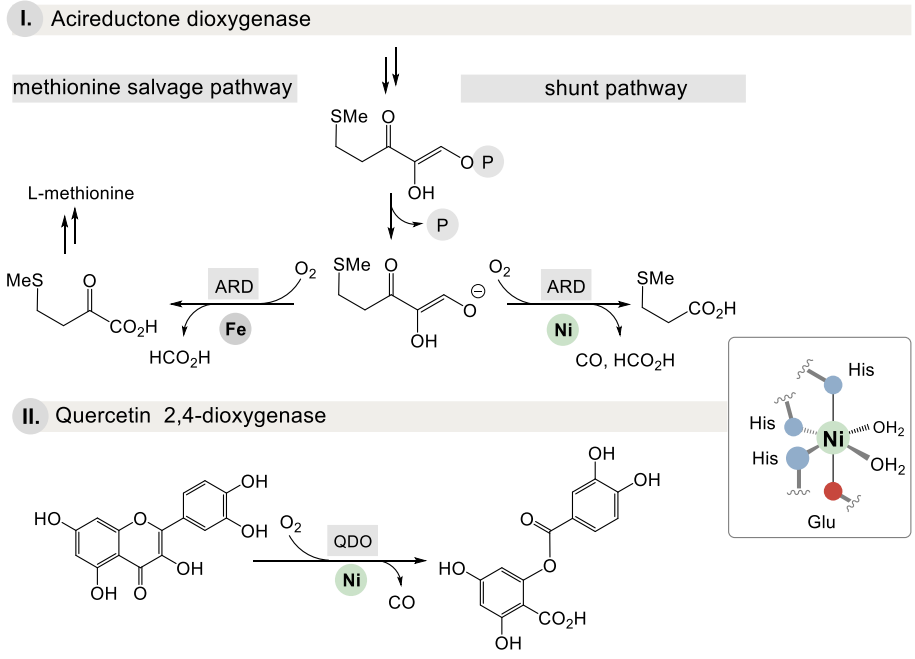

Fig. 9. Ni-based dioxygenases (ARD & QDO) and oxidations they are involved in.

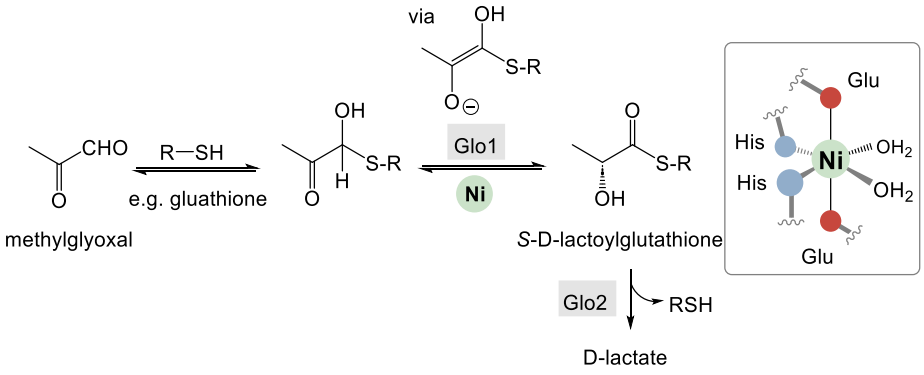

Fig. 10. Ligand sphere of Ni-dependent glyoxalase I and biotransformation it promotes.

the oxidation process; instead, the proposed mechanism suggests that the metals (either Fe or Ni) facilitate the formation of enolates. These metal-enolate intermediates then enable the addition of O2 through a one-electron transfer process.

A second example is quercetinase (QDO) that belongs to the cupin superfamily of enzymes.It is involved in the first step of aerobic breakdown of plant-derived flavonols by fungi and some bacteria. QDO is a Ni-dependent 2,4-dioxygenase that promotes the dioxygenolytic cleavage of the flavonol quercetin in which O_2 serves as oxidant. It has to be noted that the exact mechanism of this Ni supported catalysis and O_2 activation is a matter of debated up today (Wang et al., 2018) (Fig. 9.II).

However, the ligand spheres around the Ni found in ARD and QDO are very similar in that four sites of the octahedron are occupied by glutamic acid and three histidines via one of the nitrogen atoms in the histidine ring.

The composition of the ligand sphere in Fe-dependent dioxygenases is similar to that of Ni-dependent dioxygenases in that it is governed by histidine. Of particular interest in this context are the cysteine dioxygenases, where the Fe center uses O_2 to oxidize the substrate cysteine to form L-cysteine sulfinic acid. This is clear evidence that S, and in this case the thiol group, tends to oxidize when the oxygen is activated by Fe (Gao et al., 2024, Simmons et a. 2005, Ye et al., 2007).

3.3. *Ni as Lewis acid*

3.3.1. *Glyoxalase I*

Glyoxalase I (Glo1) is a Ni-dependent enzyme, absent in archaea, that is involved in the cellular detoxification of α-ketoaldehydes, specifically the metabolic by-product methylglyoxal (*Suttisansanee, U., and Honek, J. F. (2019)*). It utilizes intracellular thiols such as glutathione and these are added to α-ketoaldehydes. The intermediate *O,S*-hemiacetal supposedly undergoes an enolization, re-enolization process which provides the corresponding lactic acid thioester. In concert with glyoxalase II (Glo2) hydrolysis yields D-lactic acid. GLo1 is a metal-dependent enzyme with Zn^{2+} as cofactor (Thornalley, 1993) (Fig. 10). However, GLo1 of *Escherichia coli* (*E. coli*) depends on Ni^{2+} (Clugston et al., 1998) and seems to by typically accociated with microorganisms as well as plants (*Suttisansanee, U., and Honek, J. F. (2019)*). The coordination sphere to Ni in Glo1 is composed of two histidine and two glutamate residues and the other two sites are occupied by water. In this respect, while it is structural similar to Ni-dependent dioxygenases, the role of Ni in Glo1 is not a redox one but is clearly associated with the generation of the enolate intermediate.

3.3.2. *Ni-pincer*

Recently, a new cofactor called Ni–pincer nucleotide cofactor (NPN)

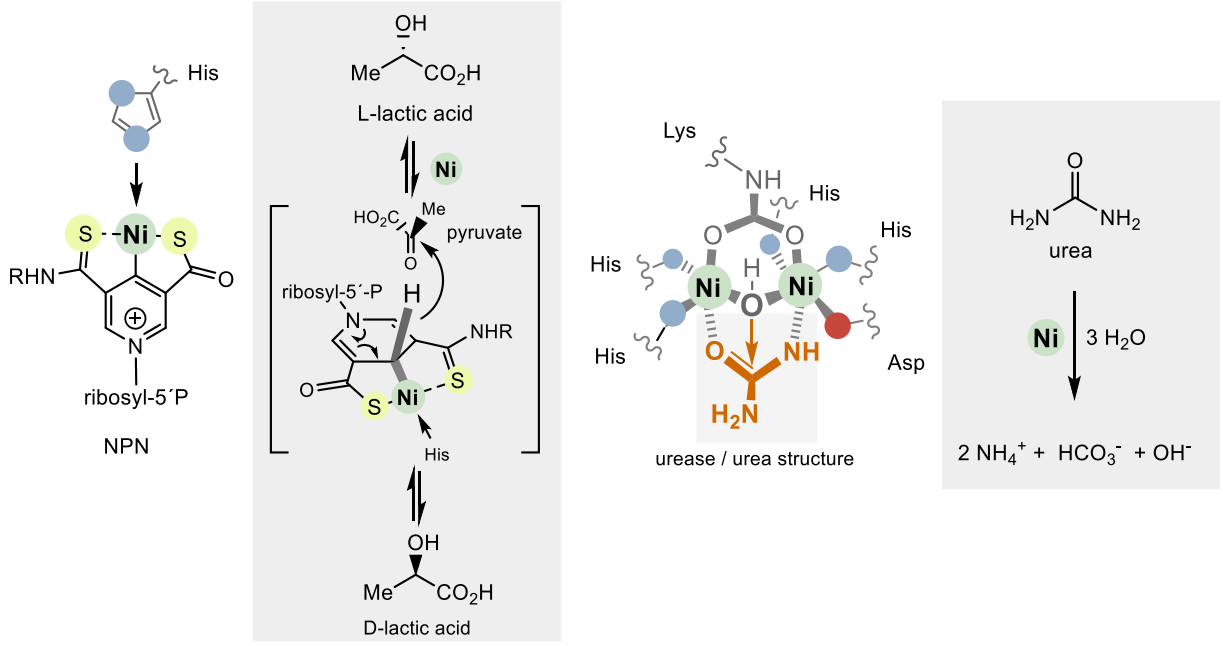

Fig. 11. Structures of Ni-pincer nucleotide (NPN) and di-Ni complex with urea bound found in ureases as well as biotransformations they promote.

was found in *Lactobacillus plantarum* which was shown to catalyze racemizations of α-hydroxycarboxylates such as lactate. The reaction is driven by NPNs ability to function as a transient hydride acceptor although the hydride transfer does not dierectly occur on Ni but as in nicotinamide NAD(P)/NAD(P)H, the biosynthetic precursor, on the heterocycle (Desguin et al., 2015 and 2016, Rankin, 2018). The cofactor is structurally unique as Ni is flanked by two S atoms that are part of a modified pyridinium ring (Fig. 11, left). Remarkably, NPN contains a carbon-Ni bond. Bioinformatics studies suggest that these newly found NPN are widely distributed in microorganisms. It will be interesting to see how large the biochemical potential of NPN actually is (Chatterjee et al., 2022). LarC is the Ni-insertase that catalyzes the insertion of Ni in the final biosynthetic step of NPN biosynthesis (Turmo, 2022). Structural data on the ligand sphere around Ni, however, are so far missing. From an evolutionary perspective this Ni cofactor must have appeared late on the stage, as its biosynthesis requires the presence of several coenzymes and cofactors, including Fe S clusters and particularly nicotinamide which provides all atoms of the pyridine ring (Kirschning, 2022a).

3.3.3. *Urease*

Urease, classified as a Ni(II) enzyme, provides a crucial process in nitrogen recycling. It is a Ni-containing metalloenzyme that catalyzes the hydrolysis of urea into ammonia (NH_3) and carbamate (H_2N-COOH), which then further decomposes spontaneously to NH_3 and carbon dioxide (CO_2) (Kappaun et al., 2018a, Callahan et al., 2005). Recycled urea comes from the breakdown of arginine and possibly purines and ureides. It occurs in bacteria, archaea, plants, fungi, algae, and invertebrates, but not in mammals. (Krajewska, 2009; Maroney and Ciurli, 2014). While predominantly produced by bacteria, fungi, and plants, (Kappaun et al., 2018b) certain archaea particularly hyperthermophilic and halophilic archaea also exhibit urease activity (Mizuki et al., 2004; Miraula et al., 2015). Sequence analyses show that the known ureases across different living species, including their catalytic domains, are highly conserved.

The enzyme's comprehensive description dates back to 1926 when James B. Sumner provided a detailed account. However, its catalytic activity had been recognized as early as 1876 by the French chemist Frédéric Alphonse Musculus, who explored urea breakdown in the absence of microorganisms but in the presence of the active enzyme, coining the term "urease."(Musculus, 1876). Although Ni plays crucial roles in many organisms (Boer et al., 2014), the first protein with a functionally significant Ni, jack bean urease, was discovered in 1975 (Walsh and Orme-Johnson, 1987). Interestingly, although urease's enzymatic activity was known for approximately 50 years before this discovery, it was only in 1975 that the Ni centers within the enzyme were identified. Jack bean urease is characterized by two Ni ions per subunit. In bacterial urease, these diatomic Ni ions are bridged by a carboxylated lysine, maintaining a Ni-Ni distance of approximately 3.26 Å (Wang et al., 1994; Carter et al., 2009). The function of the different Ni atoms have been investigated (Dixon et al., 1980). In fact, here Ni is not involved in redox chemistry, but acts as a Lewis acid. It is hypothesised that one Ni atom activates the carbonyl group in urea, whereas the other Ni atom serves to increase the nucleophilicity of water, facilitating the hydrolysis of urea by protein side chains. Support for this suggestion was recently collected from the solved structure of the elusive urease–urea complex (Mazzei et al., 2019) (Fig. 11, right).

Two main types of urease are known, one eukaryotic which is composed of a few molecules of a single polypeptide subunit and the second one found in prokaryotes composed of two or three heterogeneous subunits. Ureases from different sources share a high percentage of homology (~ 55%) between their amino acid sequences, suggesting divergence from a common ancestor (Kappaun et al. 2018). Bacterial, archaeal, plant and fungal ureases are made up of different types and/or numbers of subunits (Krajewska, 2009). Bacterial and archaeal ureases are made up of three distinct subunits (α, β and γ), commonly forming trimers $(\alpha\beta\gamma)_3$, except those of *Helicobacter* species, which are made up of two subunits (α & β) and were shown to form a dodecameric complex $((\alpha\beta)_3)_4$. In contrast, plant and fungal ureases consist of identical α subunits, typically forming homotrimers (three α subunits, "α_3") or homohexamers (six α subunits, "α_6"). These α subunits result from the fusion of the corresponding α, β, and γ subunits found in bacterial ureases (Mazzei et al., 2020). Despite still being under debate, the ancestral state for ureases have been implied to be the three-chained organization according to a study by Ligabue-Braun *et al.* in 2013 (Ligabue-Braun et al., 2013), suggesting the prokaryotic form of the enzyme to be the primitive one in relation to the eukaryotic form.

Ureases perform an array of functions, and apart from being a key component of the global nitrogen cycle (Alfano & Cavassa, 2020), as well as being the main virulence factor in a variety of human pathogenic

bacteria (Maroney and Ciurli, 2014), also show insecticidal and fungitoxic effects in plants (Kappaun et al. 2018). Another important function of ureases in nature is the promotion of calcium carbonate ($CaCO_3$) formation (Krajewska, 2009). First theorized by Campbell and Speeg in 1969 (Campbell and Speeg, 1969) for biocalcifying invertebrates and plant systems, the process occurs when ammonia (NH_3), generated from urea hydrolysis by urease, neutralizes the protons generated from the reaction of carbonic anhydrase (CA), an enzyme that catalyzes the reversible hydration of carbon dioxide (CO_2) into bicarbonate (HCO_3^-) and a proton (H^+)(Le Roy et al., 2014). Bicarbonate (HCO_3^-) then further dissociates into CO_3^{2-} and forms calcium carbonate ($CaCO_3$) in the presence of calcium ions (Ca^{2+}) facilitated by the increase in pH due to the ureolysis reaction (Krajewska, 2017). The increase in pH is a crucial factor that influences the carbonate saturation index, as well as the availability of a nucleation template (Li et al., 2015). Urease plays a key role in biologically induced mineralization (BIM), where biological activity triggers physicochemical changes in the environment, promoting mineral nucleation and growth (Bindschedler et al., 2016). This type of biomineralization is very common and mainly reported in urease-positive microbial organisms, especially prokaryotes (Chen et al., 2009, Dhami et al., 2014, Ferrer et al., 2020, Ma et al., 2020, Görgen et al. 2020, Liu et al. 2021). However, there has been a few studies indicating that urease-induced biomineralization also occurs in other urease-positive organisms, like some invertebrates, such as the gastropod mollusk *Aplysia californica* (Pedroso et al. 1997) where it was shown to be crucial for the formation of statoconia (calcium carbonate granules in the gravity-sensing organ), as well as the coral *Acropora acuminata*, where urease was shown to stimulate calcification in the tips (Crossland and Barnes, 1974), and in the land snail *Helix pomatia* L (the Roman snail), where urease appeared to be involved in the process of calcium deposition and crystal formation within the shell-repair membrane of the snail (Abolinš-Krogis, 1986). Other urease-positive organisms involved in biologically induced biomineralization are some fungi, such as *Neurospora crassa*, which was found to precipitate metal carbonates when incubated in urea-amended medium (Li et al., 2014), as well as *Pestalotiopsis* sp. and *Myrothecium gramineum*, which exhibited significant $CaCO_3$-producing abilities when grown in urea-modified media (Li et al., 2015). It has even been suggested that similar mechanisms have evolved in higher vertebrates, like hens, to enable biological $CaCO_3$ deposition during egg-laying by way of an increased production of ammonium ions (NH_4^+) (Laumer et al., 2019). The oldest nitrogen cycle (Canfield et al., 2010; Stüeken et al. 2016) where nitrogen is fixed is however not the urea cycle but instead the use of nitrogenase. This cycle does not include Ni but instead V and Mo where the Mo nitrogenase is the more common and efficient type. It is not entirely known why the nitrogenase enzyme would use V and Mo as cofactors in a world where Ni is far more common. One suggestion is that the FeMo-cofactor of nitrogenase may be less common, but much more stable and efficient, making it favourable in the selection process (Grunenberg, 2017; Rucker & Kaçar 2024). Grunenberg (2017) used quantum-mechanical calculations to demonstrate that the interstitial carbon in both the FeMo and FeV cofactors of nitrogenase is bound more tightly than previously recognized. However, MoFe nitrogenase exhibits greater strength, as the presence of molybdenum enables the formation of more stable and efficient catalytic bonds with nitrogen. This results in faster nitrogen fixation and lower energy requirements compared to other types of nitrogenases.

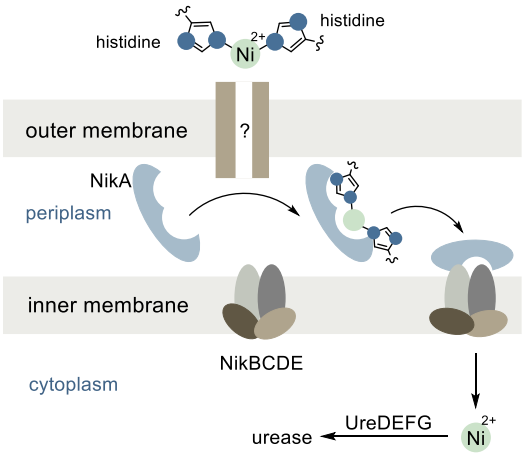

Fig. 12. Nickel trafficking in *Klebsiella pneumoniae*. Ni^{2+} is sequestered by L-histidine then passes through the outer membrane (unknown protein) into the periplasm. This is bound by NikA and transported into the cytoplasm via the NikBCDE ABC-type transporter and taken up to generate the urease system.

3.4. Other Ni-dependent proteins

3.4.1. Ni-transport

For Ni-bearing enzymes to fulfill their biological functions, Ni must be transported into the cell, a process facilitated by permeases such as HoxN, NixA, NikA, B, C, E, HupE, UreJ, and NiaX (Eitinger et al., 1997; Wolfram and Bauerfeind, 2002). There are two types of Ni transporter systems and those can be divided into primary and secondary active systems, where the Nik transporters (ABCDE, MNQO and KLMQO) belong to the former and NiCoT, UreH, HupE/UreJ and TBDT belongs to the latter (Eitinger, 2013). The two major high affinity transport systems for transferring Ni across the membrane, the Nik system (Fig. 12) and the HoxN system and both of these systems commonly involve histidine as the major binder for Ni.

Mutagenesis studies investigating the extent of Ni uptake reveal that histidine overwhelmingly dominates the overall function of the permease (Eitinger et al., 1997; Wolfram and Bauerfeind, 2002). The transport of Ni in *Helicobacter pylori*, for example, is facilitated by the permease NixA, part of a larger family of Ni-Co transporters (Wolfram and Bauerfeind, 2002). However, it is not entirely known in detail how Ni is carried across the cell membrane to the inner parts of the cells where it may be incorporated into the urease. Wolfram and Bauerfeind (2002) identified the amino acids histidine, aspartate and cysteine as the best in vivo Ni binders (but low capacity) of all amino acids and are playing a crucial role in NixA. Interestingly, some other crucial amino acids for NixA are low affinity binders (phenylalanine, serine, asparagine, and threonine) of Ni but have a high capacity to transport Ni, which was shown to be of crucial importance for the function of urease. One may speculate that both functions are important so that binding, transport and release is part of the complete functionality of a transporter permease.

Other mutagenesis studies on the Ni transport system HoxN revealed that histidine is among the best ligands of Ni to the cell (Eitinger et al., 1997). Interestingly, unlike for histidine, replacement of cysteine with alanine, did not critically influence the Ni^{2+} uptake function of the HoxN permease. Other transporter systems for other divalent cations such as Co^{2+} have additionally revealed that despite amino acid sequences similarities between Co^{2+} and Ni^{2+} uptake permeases, the ion selectivity is relatively accurate. It is still unknown what constitutes the selectivity mechanism in detail. In a study carried out by Degen and Eitinger (2002), demonstrated that the exchange of valine for phenylalanine in HoxN, increases the Ni^{2+} uptake capacity considerably. Furthermore, this mutation opened the door for Co^{2+} transport too, which may be indicative of how specificities of the amino acids work. Thus, the balance between capacity and specificity, represented by the different amino acids, are thus be the crucial separator that determine what cations are entering the cells.

3.4.2. Methanogenesis

Methanogens are particularly noteworthy from a Ni perspective as they utilize the highest amount of Ni among organisms and that they, because of that characteristic, was one of the earliest organisms on earth.

The ancient origins of methanogens are supported by both phylogenetic and geochemical evidence (Nitschke et al. 2006, Battistuzzi et al. 2004, Ueno et al. 2006). Methanogens occupy a basal position in the tree of life, suggesting that their metabolic pathways are ancient and may have been critical to early life forms, potentially even before LUCA. Nitschke et al. (2006) highlight that Ni-bearing enzymes, such as certain types of hydrogenases (described in section 3.1.2) and enzymes involved in denitrification (3.1.1), are deeply rooted in the phylogenetic tree. This suggests that these enzymes, and the metabolic pathways they support, were likely present in pre-LUCA organisms. Ueno et al. (2006) provide isotopic evidence of methane production as early as 3.5 billion years ago, found in ancient rock formations. The carbon isotopic signatures indicate that biologically mediated methanogenesis was already occurring, suggesting that methanogens and their metabolic machinery were well-established at this time, which is in line with the work by Nitschke et al. 2006, suggesting that important parts of the metabolic pathways in methanogenesis/methanotrophs predated LUCA. The reliance on Ni as a cofactor in key methanogenic enzymes also aligns with the geochemical conditions of early Earth, where Ni was abundant due to processes like serpentinization, which released H_2 and other reduced gases conducive to methanogenic activity. Nitschke et al. (2006) also point to Ni's role in early denitrification processes. While denitrification is less central to methanogens, it is a significant aspect of early anaerobic respiration. The presence of Ni-dependent enzymes in these pathways suggests that life before LUCA may have had a diverse metabolic toolkit, enabling it to exploit a range of redox reactions.

Phylogenetically older methanogens, lacking cytochromes, can reduce CO_2 into CH_4 under significantly lower H_2 partial pressure compared to cytochrome-bearing methanogens (Neubeck et al., 2016). This characteristic may be advantageous for methanogens in deep subsurface biospheres where H_2 is limited, and high H_2 pressure is thermodynamically unfavorable for the conversion of organic acids. Another advantage of cytochrome-lacking methanogens is their ability to switch hydrogenase under Ni limitation to a pure [Fe] hydrogenase, rendering them less susceptible to Ni scarcity compared to methanogens with cytochromes (Neubeck et al., 2016). This aspect holds significance when considering the "Ni famine hypothesis" (Konhauser et al., 2009, 2015, see section 2.7.1), which postulates a severe limitation of Ni in the oceans during the GOE, potentially starving methanogens and consequently reducing the global atmospheric CH_4 concentration. However, limitations in both Ni and Fe may have adverse effects on methanogen growth and CH_4 formation.

4. Prebiotic nickel

4.1. General considerations

Despite being a trace element in Earth's crust, Ni has played a crucial role in the origin and subsequent evolution of life. Maybe one of its most determining factors for microbial life was, and still is, the catalytic role it plays in the W–L pathway, which is generally considered the most ancient CO_2 fixation process. The pathway's product, acetyl-CoA, synthesized by ACS, provides a link between a primordial energy source, H_2, and the Krebs cycle, the hub of metabolism. In fact, the two central proteins in primordial bioenergy generation are Ni enzymes: hydrogenase and CODH. Before the invention of photosynthesis, energy could only be obtained locally and, thanks to volcanism and serpentinization, both H_2 and CO would have been relatively abundant sources of reducing power. Methanogens, which use parts of the W–L pathway for methanogenesis, add MCR, a fourth essential Ni enzyme, to their catalytic repertoire. But why Ni? When Ni is embedded in Fe sulfides one finds a dramatic increase of the CO_2 conversion rate.

The potential origin of life on mineral surfaces is often linked to the catalytic activity of (FeNi)S, which mimics several key biochemical reactions (see section 3.1.1, Russell and Martin). However, the presence of Ni is not unique to enzymes like Ni-containing CODH and [NiFe] hydrogenase. For instance, there are CODHs with [MoCu] active sites and Ni-free [FeFe] hydrogenases. The use of Mo and Cu in CODH can be attributed to its origin in aerobic bacteria that evolved post-GOE, when these metals became more bioavailable. The situation with [FeFe] hydrogenase, found in anaerobic organisms, is more complex. Its catalytic site appears more "mineral-like" than the [NiFe] counterpart, suggesting that the evolutionary choice of Ni may have been contingent. Thus, life may have originated in a geochemical niche, such as dry-wet cycles near volcanic or hydrothermal environments, where a local atmosphere rich in CO, H_2, H_2S, and (FeNi)S minerals, possibly including meteoritic schreibersite, prevailed. In this environment, these early catalysts would have been involved in CO_2 fixation, organic phosphorylations and polymerizations, creating the first proto-metabolic pathways and networks. The exchange of catalysts and cofactors, as well as the combination of these and other metabolic pathways arising from various mineral substrates, could have led to a global autocatalytic unit and a first manifestation for an early form of life (Kirschning, 2021; Kirschning, 2022b). Later, the appearance of the first encoded peptides would have initiated the involvement of proteins in catalysis and biocatalysis, partly associated with metals.

4.2. Nickel and schreibersite

Schreibersite, a Fe-Ni-phosphide (Fe_2NiP) mineral, is frequently found in meteorites and was first described by the Swedish chemist Jöns Jacob Berzelius in 1833. This mineral has gained significant attention in the field of prebiotic chemistry due to its potential role in the origin of life. Researchers such as Pasek and Lauretta (2005) and Bryant and Kee (2006) have proposed that schreibersite could have served as a critical source of reactive phosphorus on early Earth, facilitating the formation of phosphorylated biomolecules, which are essential for biological processes like energy transfer and signaling. Owing to their involvement in essential biochemical processes across all domains of life, these molecular entities were likely important to the development of prebiotic chemistry and the eventual emergence of life on early Earth. In aqueous environments, schreibersite has been proposed as a plausible geochemical source of reduced phosphorus species, such as phosphite, which may have played a more pivotal role in prebiotic synthesis than the thermodynamically more stable orthophosphate compounds. Importantly, the release of phosphite from schreibersite does not require elevated temperatures, increasing its relevance in origin-of-life scenarios under mild geochemical conditions.

Recent investigations, such as those by Pantaleone et al. (2022), have explored the catalytic behavior of schreibersite using quantum mechanical models, with a particular focus on the distinct interactions of Ni and Fe Fe with water. While Fe generally exhibits a higher positive charge, which would typically favor stronger water adsorption, these studies have revealed a counterintuitive result: the Ni-H_2O complex demonstrates greater stability than the analogous Fe-H_2O interaction. This observation is attributed to the unique 3d electron configuration of Ni, which allows more effective orbital overlap and bonding with the oxygen atom of water molecules, thereby stabilizing the complex. Moreover, the adsorption of water onto Ni sites induces slight modifications in coordination geometry and alters the surface charge distribution of schreibersite, potentially influencing its catalytic reactivity under prebiotic conditions.

In contrast with Fe, where the adsorption is driven by electrostatic complementarity and charge transfer, the Ni-H_2O adsorption affects the coordination geometry more than it does the electronic structure directly. The metal-O bond on the surface is also shorter for Ni than Fe, making Ni-O bond more stable than the Fe-O bond in a water loaded schreibersite surface. The stronger adsorption of water to Ni will affect also the adsorption characteristics of the neighboring Fe, showing that if three water molecules approach the schreibersite surface, only one molecule will bind to the water and the rest will attach to each other with H-bonds rather than adsorb to the Fe. These differences may

provide explanations to why Fe and Ni have such different behaviours as catalysts and pinpoints the geometrical flexibility of Ni. These characteristics of Ni with and without Fe is likely also influencing prebiotic chemistry, such as the polymerization of amino acids with schreibersite as a catalyst, due to the water binding properties and putatively an effect of stabilizing intermediates. Together with the readily released phosphite, Schreibersite may have played a crucial role in prebiotic chemistry. Phosphorylation reactions, driven by reactive phosphorus, are key steps in the prebiotic synthesis of biomolecules and these reactions could potentially aid in the activation of amino acids or other intermediates, facilitating their polymerization.

4.3. Nickel and amino acids and other privileged ligands

We chose to subdivide this review article according to the biochemical functions of Ni-dependent enzymes, starting with C1 fixation and the Wood-Ljungdahl pathway. An analysis of the ligand sphere around the central Ni reveals a change of preferred ligands over time. In an oxygen-free environment, S is the preferred atom for the formation of complexes with Ni. Later in time a transition to complexes with nitrogen bearing ligands occurred, with the amino acid histidine taking on a predominant role.

4.3.1. Ni and Cysteine

Cysteine shows a strong affinity to Ni and is fundamental in the suggested pre-LUCA enzymes CODH, ACS, urease and (Ni,Fe)-hydrogenase (Alfano & Cavassa 2020). Similar to histidine (see section 4.3.2) cysteine is equally difficlt to synthesize abiotically and numerous attempts have been pursued (Shalayel et al. 2020, Khare & Sagan 1971). Since cysteine is readily decomposed under alkaline conditions, suggested to be one of the more plausible environments for the origin of life (Gan et al. 2023), the formation rate must either be faster that the decomposition rate, the environment is not alkaline or the synthesis of cysteine is combined with some stabilizing compound. The Strecker synthesis, which is commonly referred to as one of the most prevalent and common pathways for forming amino acids (Bada et al. 2011) is seemingly not a feasible pathway for the abiotic synthesis of cysteine under plausible prebiotic conditions. However, cysteine is thought to have been a crucial component in prebiotic chemistry since it is the primary organic source of sulfide and an essential ligand in ancient Fe-S proteins. More recent attempts to synthesize cysteine have suggested that it may indeed have been present under prebiotic conditions and part of an origin of life scenario, as a secondary product of the abiotic synthesis of serine nitrile with glycolaldehyde as the cysteine precursor (Foden et al. 2020). This would thus allow for a prebiotic chemistry plausible for early, abiotic synthesis of Ni-bearing enzymatic systems such as precursor or parts of the Ni-transport system or hydrogenases etc.

4.3.2. Ni and Histidine

Histidine stands out among the 20 encoded amino acids. Despite several efforts (Maurel and Ninio, 1987; Oró et al., 1984; Shen et al., 1987; Shen et al., 1990a, 1990b, 1990c; White and Erickson, 1980) a critical analysis raises some doubts as to whether the selected reaction conditions for the abiotic synthesis of this amino acid are appropriate. Secondly, histidine has not yet been detected in carbonaceous chondrites. Only the presence of purines with an imidazole ring in meteorites has been established. Thus it very likely did not play a role during the transition from a prebiotic to an early biotic world (Kirschning, 2022b). However, histidine was most frequently discussed in the context of the evolutionary selection of the twenty encoded amino acids and the origin of the genetic code. In this context, the rationale was linked with the *hisA* and *hisF* genes. These provide some evidence for the correctness of the "retrograde" hypothesis. (Horowitz, 1945). The biosynthesis of histidine differs from all other coded amino acids in that it is the only one whose biosynthesis is based on a nucleotide (ATP) (Fani et al., 1995). And despite the fact that the biosynthesis is quite long and consists of ten linear steps all histidine-synthesizing organisms use the same unbranched pathway consisting of eight distinct proteins, encoded by eight genes (Yanai et al., 2002). The suggested evolutionary appearance of histidine synthesis pathway have been described in Fani et al. (2007) in which they show that the hisA and hisF genes have undergone a series of elongation events followed by duplication and they suggest that these events may be very ancient. The structure of hisA and hisF genes remains consistent across different organisms, suggesting an origins even predating LUCA. This ancient structure hints at their role as potentially ancestral proteins and comparisons of the HisA protein structure provide insights into the evolutionary history of these genes. Fusions involving his genes are rare in Archaea, except for hisIE in some Euryarchaeota, likely due to horizontal gene transfer (HGT) from bacteria (Fani et al., 1995; Fani et al., 2007). However, their sample sizes is still relatively small especially for the Archaea and an increased Archaeal dataset may thus change this interpretation. In enzymatic systems, the imidazole moiety of histidine frequently serves as a central component in general acid-base catalysis, typically within evolutionarily conserved catalytic triads. Its interactions with neighboring amino acid residues and coordinated metal cations are intrinsically linked to the aromaticity and basicity of the imidazole ring, facilitating a range of catalytic and structural functions.

Various in vitro studies assessing the binding strengths of amino acids and Ni have demonstrated the robust affinity of histidine to Ni (Chivers et al., 2024). This binding capability is harnessed in protein purification methodologies, particularly the "His-tag" purification chromatography method (Hochuli et al., 1988). This method leverages the strong Ni affinity of histidine by attaching histidine residues to the target protein and separating it using Ni-containing beads. The binding site in histidine, specifically the nitrogen in the imidazole group, makes solutions with pure imidazoles even stronger binders to Ni than the histidine residues in the His-tag, rendering them excellent as eluents for releasing target proteins from the beads. Histidine not only exhibits strong binding affinity to Ni but also to several other cations including Cu, Co, and Zn. Amino acid sequence similarities between Co^{2+} and Ni^{2+} transporter systems suggest accurate ion selectivity, but the detailed selectivity mechanism remains unknown. Substituting valine with phenylalanine in HoxN enhances Ni^{2+} uptake and enables Co^{2+} transport, indicating the crucial role of amino acid specificity in determining cation entry into cells.

4.3.3. Ni and tetrapyrroles

Tetrapyrroles are present in several metal bearing porphyrin and corrin cofactors. Important examples are siroheme, heme, vtamin B12 as well as in coenzyme F_{430}. Chelatases are enzymes that metalate these macrocyclic ligands because metal incorporation into these ligand systems is kinetically extremely slow. Nickel insertion into a sirohydrochlorin is also governed by a chelatase as part of the biosynthesis of cofactor F_{430} (Moore et al., 2017) and chelatases use histidne residues to bind and direct Ni to the tertrapyrrole moiety.

The biosynthesis of the tetrapyrroles moiety is thought to be a very ancient process and the relative appearance of cofactor F_{430} has been analysed by listing the coenzymes and cofactors needed to biosynthesize other members of tetrapyrrole bearing cofactors (Kirschning 22a). Uroporphyrinogen III and precorrin II the closest precursor to F_{430} are supposedly the first macrocyclic ligands of that kind that appeared during evolution. The fact that macrocylcic tetrapyrroles are very ancient ligand systems for metals including Ni is further supported by the fact that a facile synthesis under plausible prebiotic conditions was reported by Callot (Callot and Ocampo, 2000) and Lindsey (Chandrashaker et al., 2016; Lindsey et al., 2009, 2011; Soares et al., 2012; Soares et al., 2013a, 2013b) so that Ni and other metal ions could have seen complexation well before the emergence of biologically derived porphyrin systems being available for catalysts in a chemically driven prebiotic world.

5. How nickel can be incorporated into an evolutionary scenario

In the previous sections, evolutionary references were repeatedly included in the coverage on the biological significance of Ni. This mainly concerned the chemistry of Ni and prebiotically relevant reactions with this metal. In the following, we try to draw a coherent picture of the role of Ni in the framework of chemical and biological evolution. We pay particular attention to Ni complexes and the evolutionary development of the various ligand systems based on sulphur and nitrogen.

5.1. Chemical evolution and metals

Metals, whether as dissolved cations or solids, have played a key role in the geochemical and chemical evolution towards an organic and biological world (Belmonte and Mansy, 2016; Kitadai et al., 2019a, 2019b). Within the "metallome" Mn, Fe, Co, Ni, stand out and likely also Zn, and Mo (or W) were among the previliged metals. Nickel, being one of the most abundant metals on early earth, it likely had a profound effect on prebiotic reactions due to its strong catalytic role. While serpentinisation alone generates H_2 abiotically through the oxidation of Fe^{2+}, Ni (especially in combination with Fe) may have promoted prebiotic redox reactions by activating H_2 through binding to Ni, thereby significantly facilitating the prebiotic synthesis of organic molecules, much like established in the Wood-Ljungdahl pathway. The availability of H_2 would have provided a crucial reducing power for prebiotic chemistry and could have driven the formation of carbon-containing molecules, such as methane, formate, acetate and puryvate, which are all important building blocks for larger organic molecules. It is established that Ni, Co and W are of outstanding importance for first anaerobic prokaryotes and Ni (as well as W) did lose this fundamental role to some degree as more complex organisms emerged. During biological evolution Ni bearing metalloproteins appeared on the scene in which the preferred role of S was to serve as ligand atom in part of Ni complexes. Later histidine took over as preferred ligand which was accompanied with the reversal of its chemical role. These new complexes either showed reversed redox capacity or Ni started to serve as redoxneutral Lewis acid.

This development was fostered by the GOE and the rise of molecular oxygen concentration throughout many environments on planet earth. As an element primarily involved in the group transfer of hydride,

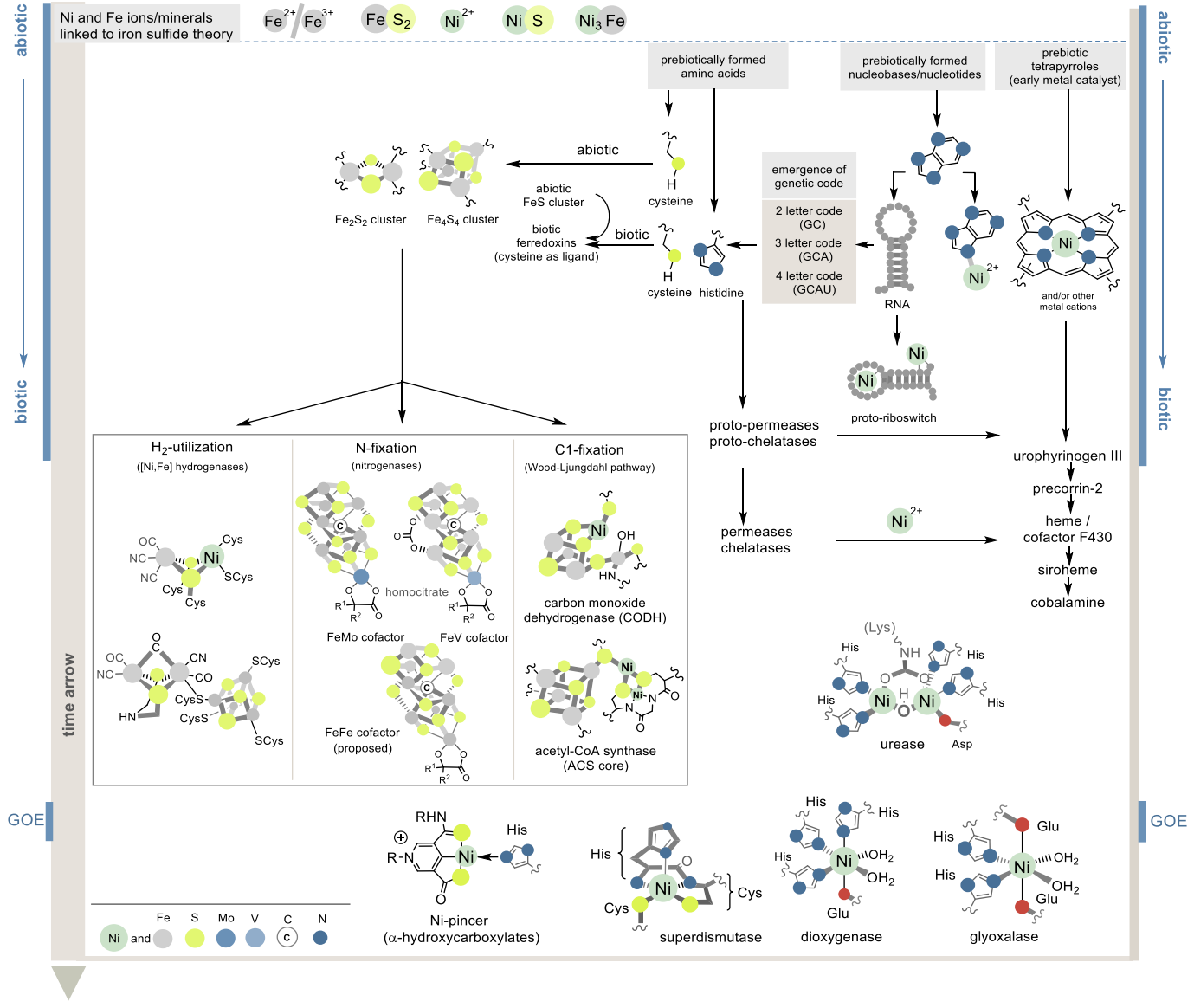

Fig. 13. The evolution of Fe and Ni catalysts from the abiotic to the biotic world with a focus on Fe/Ni-S species and the (potential) ligands histidine, cysteine, short RNAs and tetrapyrroles. The evolution of the biosynthesis of coenzymes and cofactors such as tetrapyrroles has recently been discussed (Kirschning, 2022a).

carbon monoxide and methyl, its assigned roles in aerobes and organisms with greater morphological complexity extended to dioxygen and thus to oxidation chemistry. Noteworthy, Ni-dependent enzymes have not been identified in mammals so far, which suggests that in the latest part of biological evolution Ni was „less considered“ for the devlopment of new biological functions. Thus, a story on the evolution of Ni would have to start with Ni-S (geo)chemistry and the enzymology associated with Ni complexes, especially found in aerobic organisms. From there, the nitrogen-based ligand systems and Ni will have time to come into play.

5.2. On the evolution of iron-sulfur and iron-nickel-sulfur clusters

Although we foremost cover the element Ni and its importance for key processes of life here, the question of evolution and the possible role of Ni in the transition from an abiotic to a biotic world cannot completely ignore the dominant metal Fe. Particularly remarkable is the evolutionary development from inorganic Fe-S clusters to complex core structures in fundamental and elementary processes for life. Several modified Fe-S clusters contain Ni at sites where Fe was present in (likely) predecessors. Principal catalytic mechanisms encompass the activation of molecular hydrogen as a reductant (Lubitz et al., 2014; Vignais and Billoud, 2017), alongside the coordination and stepwise reduction of carbon dioxide within the Wood–Ljungdahl pathway (Ragsdale and Pierce, 2008; Ragsdale, 2008). Only in nitrogen fixation (Burgess and Lowe, 1996; Hu et al., 2012; Raymond et al., 2004; Gruber and Galloway, 2008), the third important process for the transition from an abiotic to a prebiotic organic world, Ni has not found use. Without these processes, the development of life on Earth would have been inconceivable. The evolution of Fe and Ni catalysts and the expansion of the (bio)chemical synthetic repertoire of FeS clusters was accompanied by the development of new architectures. It is not clear whether Fe S clusters preceded mixed Fe metal clusters, especially those based on molybdenum, vanadium or Ni or whether these appeared on the stage of chemical evolution parallel. Wächtershäuser supported the former theory and called them the first "mutation" in the arena of an Fe-S world (Böchl & Wächterhäuser et al. 1992). Here, the appearance of [FeNi]-hydrogenases are of key importance (Vignais, & Billoud, 2007). This kind of ambiguity also holds for the dimerization and heterodimerization of such clusters.

The appearance of [FeNi]-hydrogenases has been linked to a different context, specifically the development of modern nitrogen-fixing molybdenum nitrogenases. Assuming that the Archean ocean contained only low concentrations of molybdenum, it can be hypothesized that instead of Mo, vanadium or Fe first played the role of molybdenum in Fe-S cluster architectures of nitrogenases (Fig. 12).

These alternative representatives, however, require considerable amounts of energy in the form of hydrogen gas to compensate for the increased requirement of moles of ATP (8 for V-nitrogenases and 32 for Fe- per catalytic cycle. Some of the released hydrogen could have been recycled by Ni-Fe hydrogenases. With the decrease in marine dissolved Ni concentrations (Konhauser et al., 2009), this energy regeneration would have been impaired. Did these geochemical changes therefore exert an evolutionary impulse on the nitrogenase system, which led to the modern, more efficient Mo nitrogenases (Fig. 13)?

Metal S clusters served as key players in organisms that belong to the first living species in an anaerobic world. This changed as oxygen species, including O_2, convert exposed Fe-S clusters into unstable forms that decompose rapidly (Imlay, 2006). The GOE consequently had an enormous impact on these catalytic systems and thus on the life that had evolved up to that point. Iron, Ni and S clusters based on these two metals are molecular showcases of evolution (Figs. 4, 6 and 13) (Camprubi et al., 2017). Wächtershäuser placed Fe sulfide (FeS_2) and later also Ni sulfides at the center of his theory (Wächtershäuser, 1988 & 1990). It attempted to explain how simple organic molecules such as the methyl thioester of acetic acid could have arisen in an inorganic world (Wächtershäuser et al. 2016). The next level of complexity of defined Fe catalysts are Fe-S [$(FeS)_n$] clusters. They are known as purely inorganic species and are also part of the thiospinel lattice of greigite displaying the cubic [4Fe4S]. These likely played a vital role as redox systems in protometabolism before LUCA (Garcia et al., 2022). Two successful attempts to create FeS cluster under plausible prebiotic conditions have been reported so far (Jordan et al., 2021; Bonfio et al., 2017). In the following, these clusters became important cofactors of many essential biological processes, initially as pure [FeS] clusters in many electron transfer processes and as donators of S e.g. for the incorporation of S in the biosynthesis of the Ni-pincer nucleotide (Hausinger et al., 2018; Chatterjee et al., 2022).

5.3. On the evolution of N-based ligand systems for nickel

A second line of discussion deals with ancient ligand systems based on nitrogen, namely histidine and tetrapyrroles, specifically early forms of prophyrins. As mentioned above, the prebiotic availability of histidine, unlike for some other proteinogenic α-amino acids (e. g. methionine, tyrosine and tryptophane) has not convincingly been proven yet (Kirschning, 2022b). It may very well be, however, that a synthetic route that leads to sensible amounts of histidine under plausible prebiotic conditions will be found in the future which would pave the way to ancient Ni-protein complexes that e.g. act as early chelatases. But in case that histidine is the result of biochemical evolution during the development of the genetic code from a two letter via a three letter to the final four letter code system, one would have to consider other N-ligands than histidine. As such nucleobases or short ancient RNA fragments could have seved as early candidates to bind Ni via nitrogen. This hypothesis would bring the RNA world theory into play. It puts paramount importance to the issue of catalysis, since RNAs, specifically ribozymes can show catalytic properties and thus allow to interfer into metabolism and expanding it. In addition metals and the emergence of metal cofactors have to be included in the evolution of catalysis (Kirschning, 2021). The RNA world theory also suggests that metals may have played a catalytic role by either covalently bound to RNA or through weaker interactions such as those found today in riboswitches (McCown et al., 2017; Sherwood and Henkin, 2016; Serganov and Patel, 2012), which gave rise to "co-ribozymes.Vestiges of such RNA conjugates that bind either metals or coenzymes are riboswitches that today have been given the role of regulation. Riboswitches are mRNAs composed of short, simple sequences. They are capable of binding metabolites and metal cations, which to chenges in the the secondary RNA structure. As such the activation and or of deactivating gene expression is affected. One known bacterial riboswitch can selectively bind Ni^{2+} and Co^{2+} in the low micromolar range (Furukawa et al., 2015), and evidence was also found that these can bind Fe (Sung and Nesbitt, 2020). Structural biological studies of the Co^{2+}/RNA complex revealed that a network of interactions exists around three out of four cations. The cation preferentially coordinates with the guanine nitrogen atom (N7) and a similar behaviour can be assumed for Ni. Noteworthy, the *N*-affinity is in contrast to the pronounced affinity of metals such as Mg^{2+} for oxygen-carrying ligands. These kind of selectivities may be regarded to have been of importance during chemical evolution and the transition phase to first forms of Life.

The assumption that various *N*-heterocycles must have existed on early Earth that potentially served as ligands was not only proven by prebiotic chemistry, but also by chemical analysis of one of the best-known extraplanetary objects, the Murchison meteorite. In addition to more than 80 different amino acids, various purines (e. g. xanthine), pyrimidines (e. g. uracil) and alkylated imidazoles were detected (Oba et al., 2019; Callahan et al., 2011; Naraoka et al., 2017).

The presence of urease in archaea and bacteria and the fact that the protein sequence of known ureases is very conserved suggest that this Ni-dependent enzyme must be ancient. It has been suggested that the urea cycle was one of the important metabolic pathways that formed

through an evolutionary pressure driven by a changing environment when terrestrial life forms evolved (Stüeken et al., 2016). The key feature was the water-preserving capacity of uric acid, which may have formed as a metabolic pathway during arid conditions, providing an evolutionary advantage. Due to the occurrence of urease in archaea and its unique role in the global nitrogen cycle, the origin of this Ni-dependent enzyme can be placed well before the GOE. It can be considered one of the first metalloenzymes to utilize histidine as a ligand. Wooldridge (2008) proposed that the pH-dependent inactivation of urease, coupled with atmospheric CO_2 partial pressure (pCO_2) and calcium carbonate deposition, may have been fundamental for at least four of the five largest mass extinctions over the past ~600 million years.

The arrival of the two Ni-dependent enzymes superoxide dismutase and dioxygenase can be clearly localized around or shortly after the major oxygen event due to their role in handling different oxygen species. In the case of dismutase, however, it can be speculated that this class of enzymes first learned to deal with other heteroatom radicals, e.g. those derived from S, and could therefore be much older (Neubeck and Freund, 2020).

The Ni-dependent glyoxalase I and the Ni pincer (NPN) cofactor cannot be precisely classified in terms of their arrival. This is also attributable to the fact that, as in the case of NPN, little is known about the full spectrum of its biochemical role. Considering their metabolic role in general, one would expect them to have appeared on the biological scene at a later stage.

6. Concluding remarks

This report emphasises the special significance of Ni in the early days of the development of life on planet Earth. The metal has commonly played a minor role in considerations on chemical and biological evolution alongside the very dominant Fe. However, it is obviously undisputed that it is essential for a number of very ancient anaerobic organisms living under extreme conditions, because it exerts a special ability to bind and process gases such as H_2 and CO. Hydrogenases as well as the orchestration of the Wood-Ljungdahl pathway are key field where Ni is essential. This ability appears to be related to the ligand atom sulphur, whose role in the dramatic changes that took place in the atmosphere during the GOE was challenged by the now oxidative conditions and histidine progressively stepped in as a ligand for Ni as for other transition metals. Now Ni-based enzymes became involved in oxygen-dependent processes or the Ni acted as a Lewis acid.

With this report, we hope to have brought the special role of Ni in evolution more into the spotlight and inspire thoughts on the origin of life.

Declaration of competing interest

The authors declare that they have no known competing financial interests or personal relationships that could have appeared to influence the work reported in this paper.

Acknowledgement

AK thanks the Wenner-Gren Foundation for funding a sabbatical stay at Uppsala University (Sweden). The foundation helped to establish a collaboration between AK ans AN. A.N. thanks the Swedish research council (VR) project to A.N. (#2017-05018) and the Swedish National Space board (DNR 13/100).

Data availability

No data was used for the research described in the article.

References

Abolinš-Krogis, A., 1986. The effect of carbonic anhydrase, urea and urease on the calcium carbonate deposition in the shell-repair membrane of the snail, Helix pomatia L. Cell Tissue Res. 244, 655–660. https://doi.org/10.1007/BF00212546.
Alfano, M., Cavazza, C., 2020. Structure, function, and biosynthesis of nickel-dependent enzymes. Protein Sci. 29, 1071–1089. https://doi.org/10.1002/pro.3836.
Ananikov, S.P., 2015. Nickel: the “Spirited Horse” of transition metal catalysis. ACS Catal. 5, 1964–1971. https://doi.org/10.1021/acscatal.5b00072.
Bada, J., 2011. Strecker Synthesis. In: Gargaud, M., et al. (Eds.), Encyclopedia of Astrobiology. Springer, Berlin, Heidelberg.. https://doi.org/10.1007/978-3-642-11274-4_1527
Bauer, S., Blomqvist, S., Ingri, J., 2017. Distribution of dissolved and suspended particulate molybdenum, vanadium, and tungsten in the Baltic Sea. Marine Chem. 196, 135–147. https://doi.org/10.1016/j.marchem.2017.08.010.
Belmonte, L., Mansy, S.S., 2016. Metal catalysts and the origin of life. Elements 12, 413–418. https://doi.org/10.2113/gselements.12.6.413.
Beyazay, T., Martin, W.F., Tüysüz, T., 2023b. Direct synthesis of formamide from CO_2 and H_2O with nickel–iron nitride heterostructures under mild hydrothermal conditions. J. Am. Chem. Soc. 145, 19768–19779. https://doi.org/10.1021/jacs.3c05412.
Bindschedler, S., Cailleau, G., Verrecchia, E., 2016. Role of fungi in the biomineralization of calcite. Minerals 6, 41. https://doi.org/10.3390/min6020041.
Blokesch, M., Albracht, S.P.J., Matzanke, B.F., Drapal, N.M., Jacobi, A., Böck, A., 2004. The complex between hydrogenase-maturation proteins HypC and HypD is an intermediate in the supply of cyanide to the active site iron of [NiFe]-hydrogenases. J. Mol. Biol. 344, 155–167. https://doi.org/10.1016/j.jmb.2004.09.040.
Blondin, S., Bravo, E., Timmes, F.X., Dessart, L., Hillier, D.J., 2022. Stable nickel production in type Ia supernovae: A smoking gun for the progenitor mass? A&A 660. https://doi.org/10.1051/0004-6361/202142323. A96.
Bonfio, C., Valer, L., Scintilla, S., Shah, S., Evans, D.J., Jin, L., Szostak, J.W., Sasselov, D. D., Sutherland, J.D., Mansy, S.S., 2017. UV-light-driven prebiotic synthesis of iron–sulfur clusters. Nat. Chem. 9, 1229–1234. https://doi.org/10.1038/nchem.2817.
Britten, R., 2017. Regional metallogeny and genesis of a new deposit type—disseminated awaruite (Ni_3Fe) mineralization hosted in the cache creek terrane. Econ. Geol. 112, 517–550. https://doi.org/10.2113/econgeo.112.3.517.
Bruland, Kenneth W., 1980. Oceanographic distributions of cadmium, zinc, nickel, and copper in the North Pacific. Earth Planet. Sci. Lett. 47 (2), 176–198. https://doi.org/10.1016/0012-821X(80)90035-7. ISSN 0012-821X.
Bryant, D.E., Kee, T.P., 2006. Chem. Commun. 2344–2346.
Burgess, B.K., Lowe, D.J., 1996. Mechanism of molybdenum nitrogenase. Chem. Rev. 96, 2983–3012. https://doi.org/10.1021/cr950055x.
Callahan, B.P., Yuan, Y., Wolfenden, R., 2005. The burden borne by urease. J. Am. Chem. Soc. 127, 10828–10829. https://doi.org/10.1021/ja0525399.
Callahan, M.P., Smith, K.E., Cleaves II, H.J., Ruzicka, J., Stern, J.C., Glavin, D.P., House, C.H., Dworkin, J.P., 2011. Carbonaceous meteorites contain a wide range of extraterrestrial nucleobases. Proc. Natl Acad. Sci. USA 108, 13995–13998. https://doi.org/10.1073/pnas.1106493108.
Callot, H.J., Ocampo, R., 2000. In: Kadish, K., Smith, K.M., Guilard, R. (Eds.), The porphyrin handbook, 1. Academic Press, San Diego, pp. 349–398.
Cameron, V., 2009. A Biomarker Based on the Stable Isotopes of Nickel. Proc. Nat. Acad. Sci. doi. https://doi.org/10.1073/pnas.0900726106.
Cameron, V., Vance, D., 2014. Heavy nickel isotope compositions in rivers and the oceans. Geochim. Cosmochim. Acta 128, 195–211. https://doi.org/10.1016/j.gca.2013.12.007.
Cammack, R., Frey, M., Robson, R., 2001. Hydrogen as a fuel, Learning from Nature. Taylor & Francis Inc., London.
Campbell, J.W., Speeg, K.V., 1969. Ammonia and biological deposition of calcium carbonate. Nature 224, 725–726. https://doi.org/10.1038/224725a0.
Camprubi, E., Jordan, S.F., Vasiliadou, R., Lane, N., 2017. Iron catalysis at the origin of life. IUBMB Life 69, 373–381. https://doi.org/10.1002/iub.1632.
Canfield, D.E., Glazer, A.N., Falkowski, P.G., 2010. The evolution and future of earth’s nitrogen cycle. Science 330, 192–196. https://doi.org/10.1126/science.1186120.
Carter, E.L., Flugga, N., Boer, J.L., Mulrooney, S.B., Hausinger, R.P., 2009. Interplay of metal ions and urease. Metallomics: integrated biometal science 1, 207–221. https://doi.org/10.1039/b903311d.
Chandrashaker, V., Ptaszek, M., Taniguchi, M., Lindsey, J.S., 2016. Synthesis of diverse acyclic precursors to pyrroles for studies of prebiotic routes to tetrapyrrole macrocycles. New. J. Chem. 40, 8786–8808. https://doi.org/10.1039/C6NJ02048H.
Chatterjee, S., Gatreddi, S., Gupta, S., Nevarez, J.L., Rankin, J.A., Turmo, A., Hu, J. Hausinger, 2022. Unveiling the mechanisms and biosynthesis of a novel nickel-pincer enzyme. Biochem. Soc. Trans. 50, 1187–1196. https://doi.org/10.1042/BST20220490.
Chen, L., Shen, Y., Xie, A., Huang, B., Jia, R., Guo, R., Tang, W., 2009. Bacteria-mediated synthesis of metal carbonate minerals with unusual morphologies and structures. Crystal Growth & Design 9, 743–754. https://doi.org/10.1021/cg800224s.
Chivers, P.T., Basak, P., Maroney, M.J., 2024. One His, two His the emerging roles of histidine in cellular nickel trafficking. J. Inorg. Biochem. 259, 112668. https://doi.org/10.1016/j.jinorgbio.2024.112668.
Clayton, D.D., 1983. Principles of Stellar Evolution and Nucleosynthesis *(reprinted.)*. University of Chicago Press, Chicago, IL. Chapter 7, ISBN 978-0-226-10952-7.
Clayton, D.D., Fowler, W.A., Hull, T.E., Zimmerman, B.A., 1961. Neutron capture chains in heavy element synthesis. Annals of Physics 12, 331–408. https://doi.org/10.1016/0003-4916(61)90067-7.

Clugston, S.L., Barnard, J.F.L., Kinach, R., Miedema, D., Ruman, R., Daub, E., Honek, J. F., 1998. Overproduction and characterization of a dimeric non-zinc glyoxalase I from Escherichia coli: evidence for optimal activation by nickel ions. Biochemistry 37, 8754–8763. https://doi.org/10.1021/bi972791w.

Crossland, C.J., Barnes, D.J., 1974. The role of metabolic nitrogen in coral calcification. Marine Biol. 28, 325–332. https://doi.org/10.1007/BF00388501.

Degen, O., Eitinger, T., 2002. Substrate specificity of nickel/cobalt permeases: insights from mutants altered in transmembrane domains I and II. J. Bacteriol. 184, 3569–3577. https://doi.org/10.1128/JB.184.13.3569-3577.2002.

Dekov, V., 2006. Native nickel in the TAG hydrothermal field sediments (Mid-Atlantic Ridge, 26°N): Space trotter, guest from mantle, or a widespread mineral, connected with serpentinization? J. Geophys. Res. Solid Earth 111, B05103. https://doi.org/10.1029/2005JB003955.

Desguin, B., Zhang, T., Soumillion, P., Hols, P., Hu, J., Hausinger, R.P., 2015. Tethered niacin-derived pincer complex with a nickel-carbon bond in lactate racemase. Science 349, 66–69. https://doi.org/10.1126/science.aab2272.

Deshpande, A.R., Pochapsky, T.C., Ringe, D., 2017. The metal drives the chemistry: dual functions of acireductone dioxygenase. Chem. Rev. 117, 10474–10501. https://doi.org/10.1021/acs.chemrev.7b00117.

Dhami, N.K., Reddy, M.S., Mukherjee, A., 2014. Synergistic role of bacterial urease and carbonic anhydrase in carbonate mineralization. Appl. Biochem. Biotechnol. 172, 2552–2561. https://doi.org/10.1007/s12010-013-0694-0.

Dherbassy, Q., Mayer, R.J., Muchowska, K.B., Moran, J., 2023. Metal-pyridoxal cooperativity in nonenzymatic transamination. J. Am. Chem. Soc. 145, 13357–13370. https://doi.org/10.1021/jacs.3c03542.

Dixon, N.E., Riddles, P.W., Gazzola, C., Blakeley, R.L., Zerner, B., 1980. Jack bean urease (EC 3.5.1.5). V. On the mechanism of action of urease on urea, formamide, acetamide, N-methylurea, and related compounds. Canad. J. Biochem. 58, 1335–1344. https://doi.org/10.1139/o80-181.

Drennan, C.L., Heo, J., Sintchak, M.D., Schreiter, E., Ludden, P.W., 2001. Life on carbon monoxide: X-ray structure of Rhodospirillum rubrum Ni-Fe-S carbon monoxide dehydrogenase. Proc. Natl. Acad. Sci. U. S. A. 98, 11973–11978. https://doi.org/10.1073/pnas.211429998.

Dupont, C.L., Barbeau, K., Palenik, B., 2008a. Ni uptake and limitation in marine Synechococcus strains. Appl. Environ. Microbiol. 74 (1), 23–31. https://doi.org/10.1128/AEM.01007-07.3.

Dupont, C.L., Neupane, K., Shearer, J., Palenik, B., 2008b. Diversity, function and evolution of genes coding for putative Ni-containing superoxide dismutases. Environ. Microbiol. 10 (7), 1831–1843. https://doi.org/10.1111/j.1462-2920.2008.01604.x.

Edwards, K., Glazer, B., Rouxel, O., Bach, W., Emerson, D., Davis, R.E., Toner, B.M., Chan, C.S., Tebo, B.M., Staudigel, H., Moyer, C.L., 2011. Ultra-diffuse hydrothermal venting supports Fe-oxidizing bacteria and massive umber deposition at 5000 m off Hawaii. ISME J 5, 1748–1758. https://doi.org/10.1038/ismej.2011.48.

Eitinger, T., 2013. Nickel Transporters. In: Kretsinger, R.H., Uversky, V.N., Permyakov, E.A. (Eds.), Encyclopedia of Metalloproteins. Springer, New York, NY, pp. 1515–1519. https://doi.org/10.1007/978-1-4614-1533-6_85.

Eitinger, T., Wolfram, L., Degen, O., Anthon, C., 1997. A Ni^{2+} binding motif is the basis of high affinity transport of the alcaligenes eutrophus nickel permease. J. Biol. Chem. 272, 17139–17144. https://doi.org/10.1074/jbc.272.27.17139.

Estrade, N., Cloquet, C., Echevarria, G., Sterckeman, T., Deng, T., Tang, Y., Morel, J.-L., 2015. Weathering and vegetation controls on nickel isotope fractionation in surface ultramafic environments (Albania). Earth Planet. Sci. Lett. 423, 24–35. https://doi.org/10.1016/j.epsl.2015.04.018.

Evans, D.J., 2005. Chemistry relating to the nickel enzymes CODH and ACS. Coord. Chem. Rev. 249, 1582–1595. https://doi.org/10.1016/j.ccr.2004.09.012.

Evans, P.N., Boyd, J.A., Leu, A.O., Woodcroft, B.J., Parks, D.H., Hugenholtz, P., Tyson, G. W., 2019. An evolving view of methane metabolism in the Archaea. Nat. Rev. Microbiol. 17, 219–232. https://doi.org/10.1038/s41579-018-0136-7.

Fakhraee, M., Hancisse, O., Canfield, D.E., Crowe, S.A., Katsev Proterozoic, S., 2019. Seawater sulfate scarcity and the evolution of ocean–atmosphere chemistry. Nature Geosci. 12, 375–380. https://doi.org/10.1038/s41561-019-0351-5.

Fakhraee, M., Crockford, P.W., Bauer, K.W., Pasquier, V., Sugiyama, I., Katsev, S., Raven, M.R., Gomes, M., Philippot, P., Crowe, S.A., Tarhan, L.G., Lyons, T.W., Planavsky, N., 2024. The history of Earth's sulfur cycle. Nature Rev. Earth Environ. https://doi.org/10.1038/s43017-024-00615-0.

Fani, R., Liò, P., Lazcano, A., 1995. Molecular evolution of the histidine biosynthetic pathway. J. Mol. Evol. 41, 760–774. https://doi.org/10.1007/BF00173156.

Fani, F., Brilli, M., Fondi, M., Lió, P., 2007. The role of gene fusions in the evolution of metabolic pathways: the histidine biosynthesis case. BMC Evol.Biol. 7 (Suppl. 2), S4. https://doi.org/10.1186/1471-2148-7-S2-S4.

Ferrer, F.M., Hobart, K., Bailey, J.V., 2020. Field detection of urease and carbonic anhydrase activity using rapid and economical tests to assess microbially induced carbonate precipitation. Microb. Biotechnol. 13, 1877–1888. https://doi.org/10.1111/1751-7915.13630.

Fleischmann, S., Du, J., Chatterjee, A., McManus, J., Iyer, S.D., Amonkar, A., Vance, D., 2023. The nickel output to abyssal pelagic manganese oxides: a balanced elemental and isotope budget for the oceans. Earth Planet. Sci. Lett. 619, 118301. https://doi.org/10.1016/j.epsl.2023.118301.

Foden, Callum S., et al., 2020. Prebiotic synthesis of cysteine peptides that catalyze peptide ligation in neutral water. Science 370, 865–869. https://doi.org/10.1126/science.abd5680.

Früh-Green, G.L., Kelley, D.S., Bernasconi, S.M., Karson, J.A., Ludwig, K.A., Butterfield, D.A., Boschi, C., Proskurowski, G., 2003. 30,000 years of hydrothermal activity at the lost city vent field. Science (New York, N.Y.) 301 (5632), 495–498. https://doi.org/10.1126/science.1085582.

Fujishiro, T., Ogawa, S., 2021. The nickel-sirohydrochlorin formation mechanism of the ancestral class II chelatase CfbA in coenzyme F430 biosynthesis. Chem. Sci. 12, 2172–2180. https://doi.org/10.1039/D0SC05439A.

Furukawa, K., Ramesh Zhou, Z., Weinberg, Z., Vallery, T., Winkler, W.C., Breaker, R.R., 2015. Bacterial riboswitches cooperatively bind Ni^{2+} or Co^{2+} ions and control expression of heavy metal transporters. Molecular Cell 57, 1088–1098. https://doi.org/10.1016/j.molcel.2015.02.009.

Gall, L., Williams, H., Siebert, C., Halliday, A., 2012. Determination of mass-dependent variations in nickel isotope compositions using double spiking and MC-ICPMSJ. Anal. At. Spectrom. 27 (1), 137–145.

Gall, L., Williams, H.M., Siebert, C., Halliday, A.N., Herrington, R.J., Hein, J.R., 2013. Nickel isotopic compositions of ferromanganese crusts and the constancy of deep ocean inputs and continental weathering effects over the cenozoic. Earth Planet. Sci. Lett. 375 ??. https://doi.org/10.1016/j.epsl.2013.05.019.

Galoisy, L., 1998. Nickel. In: Geochemistry. Encyclopedia of Earth Science. Springer, Dordrecht. https://doi.org/10.1007/1-4020-4496-8_211.

Gao, Y., Zhu, Y., Awakawa, T., Abe, I., 2024. Unusual cysteine modifications in natural product biosynthesis. RSC Chem Biol. 5. https://doi.org/10.1039/d4cb00020j, 293-231.

Garcia, P.S., D'Angelo, F., Ollagnier-de Choudens, S., Dussouchaud, M., Bouveret, E., Gribaldo, S., Barras, F., 2022. An early origin of Iron-Sulfur cluster biosynthesis machineries before Earth oxygenation. Nat. Ecol. Evol. 6, 1564–1572. https://doi.org/10.1038/s41559-022-01857-1.

Gruber, N., Galloway, J.N., 2008. An Earth-system perspective of the global nitrogen cycle. Nature 451, 293–296. https://doi.org/10.1038/nature06592.

Grunenberg, J., 2017. The interstitial carbon of the nitrogenase FeMo cofactor is far better stabilized than previously assumed. Angew. Chem. Int. Ed. 56, 7288–7291. https://doi.org/10.1002/anie.201701790.

Gueguen, B., Rouxel, O., Ponzevera, E., Bekker, A., Fouquet, Y., 2013. Nickel isotope variations in terrestrial silicate rocks and geological reference materials measured by MC-ICP-MS. Geostand. Geoanalyt. Res. 37, 297–317. https://doi.org/10.1111/j.1751-908X.2013.00209.x.

Gueguen, Bleuenn, Rouxel, Olivier, Rouget, Marie-Laure, Bollinger, Claire, Ponzevera, Emmanuel, Germain, Yoan, Fouquet, Yves, 2016. Comparative geochemistry of four ferromanganese crusts from the pacific ocean and significance for the use of Ni isotopes as paleoceanographic tracers. Geochim. Cosmochim. Acta 189, 214–235. https://doi.org/10.1016/j.gca.2016.06.005.

Gueguen, B., Rouxel, O., Fouquet, Y., 2021. Nickel isotopes and rare earth elements systematics in marine hydrogenetic and hydrothermal ferromanganese deposits. Chem. Geol. 560, 119999. https://doi.org/10.1016/j.chemgeo.2020.119999.

Hall, A., 1987. Igneous Petrology. Igneous Petrology. Longman Scientific & Technical, Harlow.

Hausinger, R.P., Desguin, B., Fellner, M., Rankin, J.A., Hu, J., 2018. Nickel–pincer nucleotide cofactor. Curr. Opin. Chem. Biol. 47, 18–23. https://doi.org/10.1074/jbc.RA118.003741.

Hazen, Robert M., Papineau, Dominic, Bleeker, Wouter, Downs, Robert T., Ferry, John M., McCoy, Timothy J., Sverjensky, Dimitri A., Yang, Hexiong, 2008. Review Paper. Mineral evolution. American Mineralogist 93 (11-12), 1693–1720. https://doi.org/10.2138/am.2008.2955.

Heinen, W., Lauwers, A.M., 1996. Organic sulfur compounds resulting from the interaction of iron sulfide, hydrogen sulfide and carbon dioxide in an anaerobic aqueous environment. Orig. Life Evol. Biosph. 26, 131–150. https://doi.org/10.1007/BF01809852.

Hiebert, R.S., Bekker, A., Houlé, M.G., Rouxel, O.J., 2022. Nickel isotope fractionation in komatiites and associated sulfides in the hart deposit, Late Archean Abitibi Greenstone Belt, Canada. Chem. Geol. 603, 120912. https://doi.org/10.1016/j.chemgeo.2022.120912. ISSN 0009-2541.

Hochuli, E., Bannwarth, W., Döbeli, H., Gentz, R., Stüber, D., 1988. Genetic approach to facilitate purification of recombinant proteins with a novel metal chelate adsorbent. Bio/Technology 6, 1321–1325. https://doi.org/10.1038/nbt1188-1321.

Hofmann, A., Bekker, A., Dirks, P., et al., 2014. Comparing orthomagmatic and hydrothermal mineralization models for komatiite-hosted nickel deposits in Zimbabwe using multiple-sulfur, iron, and nickel isotope data. Miner Deposita 49, 75–100. https://doi.org/10.1007/s00126-013-0476-1.

Holm, N.G., Oze, C., Mousis, O., Waite, J.H., Guilbert-Lepoutre, A., 2015. Serpentinization and the Formation of H_2 and CH_4 on Celestial Bodies (Planets, Moons, Comets). Astrobiology 15, 7. https://doi.org/10.1089/ast.2014.1188.

Horowitz, N.H., 1945. On the evolution of biochemical syntheses. Proc. Natl. Acad. Sci. U. S. A. 31, 153–157. https://doi.org/10.1073/pnas.31.6.153.

Hu, Y., Lee, C.C., Ribbe, M.W., 2012. Vanadium nitrogenase: A two-hit wonder? Dalton Trans. 41, 1118–1127. https://doi.org/10.1039/c1dt11535a.

Hudson, R., de Graaf, R., Rodin, M.S., Ohno, A., Lane, N., McGlynn, S.E., Yamada, Y.M. A., Nakamura, R., Barge, L.M., Braun, D., Sojo, V., 2020. CO_2 reduction driven by a pH gradient. Proc. Nat. Acad. Sci. USA 117, 22873–22879. https://doi.org/10.1073/pnas.2002659117.

Imlay, J.A., 2006. Iron-sulphur clusters and the problem with oxygen. Mol. Microbiol. 59, 1073–1082. https://doi.org/10.1111/j.1365-2958.2006.05028.x.

Jordan, S.F., Ioannou, I., Rammu, H., Halpern, A., Bogart, L.K., Ahn, M., Vasiliadou, R., Christodoulou, J., Maréchal, A., Lane, N., 2021. Spontaneous assembly of redox-active iron-sulfur clusters at low concentrations of cysteine. Nat. Commun. 12, 592. https://doi.org/10.1038/s41467-021-26158-2.

Kappaun, K., Piovesan, A.R., Carlini, C.R., Ligabue-Braun, R., 2018. Ureases: Historical aspects, catalytic, and non-catalytic properties – A review. J. Adv. Res. 13, 3–17. https://doi.org/10.1016/j.jare.2018.05.010.

Kaur, H., Rauscher, S.A., Werner, E., Song, Y., Yi, J., Kazöne, W., Martin, W.F., Tüysüz, H., Moran, J., 2024. A prebiotic Krebs cycle analog generates amino acids

with H_2 and NH_3 over nickel. Chem 10, 1528–1540. https://doi.org/10.1016/j.chempr.2024.02.001.
Keller, M.A., Kampjut, D., Harrison, S.A., Ralser, M., 2017. Sulfate radicals enable a non-enzymatic Krebs cycle precursor. Nat Ecol Evol. 1, 0083. https://doi.org/10.1038/s41559-017-0083.
Kelley, D., Karson, J., Blackman, D., et al., 2001. An off-axis hydrothermal vent field near the Mid-Atlantic Ridge at 30° N. Nature 412, 145–149. https://doi.org/10.1038/35084000.
Kelley, D.S., Karson, J.A., Früh-Green, G.L., Yoerger, D.R., Shank, T.M., Butterfield, D.A., Hayes, J.M., Schrenk, M.O., Olson, E.J., Proskurowski, G., Jakuba, M., Bradley, A., Larson, B., Ludwig, K., Glickson, D., Buckman, K., Bradley, A.S., Brazelton, W.J., Roe, K., Elend, M.J., Sylva, S.P., 2005. A serpentinite-hosted ecosystem: the Lost City hydrothermal field. Science (New York, N.Y.) 307 (5714), 1428–1434. https://doi.org/10.1126/science.1102556.
Khare, B., Sagan, C., 1971. Synthesis of Cystine in Simulated Primitive Conditions. Nature 232, 577–579. https://doi.org/10.1038/232577a0.
Kirschning, A., 2021. Coenzymes and their role in the evolution of Life. Angew. Chem. Int Ed. 60, 6242–6269. https://doi.org/10.1002/anie.201914786.
Kirschning, A., 2022a. On the evolution of coenzyme biosynthesis. Nat. Prod. Rep. 39, 2175–2199. https://doi.org/10.1039/D2NP00037G.
Kirschning, A., 2022b. On the evolutionary history of the twenty encoded amino acids. Chem. Eur. J. e202201419. https://doi.org/10.1002/chem.202201419.
Kirschning, A., 2024. Why pyridoxal phosphate could be a functional predecessor of thiamine pyrophosphate and speculations on a primordial metabolism. RSC Chem. Biol. 5, 508–517. https://doi.org/10.1039/D4CB00016A.
Kitadai, N., Nakamura, R., Yamamoto, M., Takai, K., Yoshida, N., Oono, Y., 2019a. Metals likely promoted protometabolism in early ocean alkaline hydrothermal systems. Science Adv. 5, eaav7848. https://doi.org/10.1126/sciadv.aav784.
Kitadai, N., Nakamura, R., Yamamoto, M., Takai, K., Yoshida, N., Yoshi Oono, N., 2019b. Metals likely promoted protometabolism in early ocean alkaline hydrothermal systems. Science Adv. 5, eaav7848. https://doi.org/10.1126/sciadv.aav7848.
Kitadai, N., Nakamura, R., Yamamoto, M., Okada, S., Takahagi, W., Nakano, Y., Takahashi, Y., Takai, K., Oono, Y., 2021. Thioester synthesis through geoelectrochemical CO_2 fixation on Ni sulfides. Commun. Chem. 4, 37. https://doi.org/10.1038/s42004-021-00475-5.
Kitadai, N., Shibuya, T., Ueda, H., Tasumi, E., Okada, S., Takai, K., 2024. Supercritical carbon dioxide likely served as a prebiotic source of methanethiol in primordial ocean hydrothermal systems. Commun. Earth Environ. 5. https://doi.org/10.1038/s43247-024-01689-w. Article number: 539.
Klaver, Martijn, Ionov, Dmitri A., Takazawa, Eiichi, Elliott, Tim, 2020. The non-chondritic Ni isotope composition of Earth's mantle. Geochimica et Cosmochimica Acta 268, 405–421. https://doi.org/10.1016/j.gca.2019.10.017.
Klein, F., Bach, W., 2009. Fe-Ni-Co-O-S phase relations in peridotite-seawater interactions. J. Petrol. 50, 37–59. https://doi.org/10.1093/petrology/egn071.
Konhauser, K.O., Pecoits, E., Lalonde, S.V., Papineau, D., Nisbet, E.G., Barley, M.E., Arndt, N.T., Zahnle, K., Kamber, B.S., 2009. Oceanic nickel depletion and a methanogen famine before the Great Oxidation Event. Nature 458, 750–753. https://doi.org/10.1038/nature07858.
Konhauser, K.O., Robbins, L.J., Pecoits, E., Peacock, C., Kappler, A., Lalonde, S.V., 2015. The Archean nickel famine revisited. Astrobiology 15, 804–815. https://doi.org/10.1089/ast.2015.1301.
Krajewska, B., 2009. Ureases I. Functional, catalytic and kinetic properties: A review. J. Mol. Catal. B: Enzymatic 59, 9–21. https://doi.org/10.1016/j.molcatb.2009.01.003.
Krajewska, B., 2017. Urease-aided calcium carbonate mineralization for engineering applications: A review. J. Adv. Res. 13, 59–67. https://doi.org/10.1016/j.jare.2017.10.009.
Laumer, C.E., Fernández, R., Lemer, S., Combosch, D., Kocot, K.M., Riesgo, A., Andrade, S.C.S., Sterrer, W., Sørensen, M.V., Giribet, G., 2019. Revisiting metazoan phylogeny with genomic sampling of all phyla. Proc. R. Soc. B. 286, 20190831. https://doi.org/10.1098/rspb.2019.0831.
Le Roy, N., Jackson, D.J., Marie, B., Ramos-Silva, P., Marin, F., 2014. The evolution of metazoan α-carbonic anhydrases and their roles in calcium carbonate biomineralization. Front. Zool. 11, 75. https://doi.org/10.1186/s12983-014-0075-8.
Li, Q., Csetenyi, L., Gadd, G.M., 2014. Biomineralization of metal carbonates by neurospora crassa. Environ. Sci. Technol. 48, 14409–14416. https://doi.org/10.1021/es5042546.
Li, Q., Csetenyi, L., Paton, G.I., Gadd, G.M., 2015. $CaCO_3$ and $SrCO_3$ bioprecipitation by fungi isolated from calcareous soil. Environ. Microbiol. 17, 3082–3097. https://doi.org/10.1111/1462-2920.12954.
Li, M., Grasby, S.E., Wang, S.-J., Zhang, X., Wasylenki, L.E., Xu, Y., Sun, M.S., Beauchamp, B., Hu, D., Shen, Y., 2021. Nickel isotopes link Siberian Traps aerosol particles to the end-Permian mass extinction. Nat. Commun. 12, 2024. https://doi.org/10.1038/s41467-021-22066-7.
Ligabue-Braun, R., Andreis, F.C., Verli, H., Carlini, C.R., 2013. 3-to-1: unraveling structural transitions in ureases. Naturwissenschaften 100, 459–467. https://doi.org/10.1007/s00114-013-1045-2.
Lindsey, J.S., Ptaszek, M., Taniguchi, M., 2009. Simple formation of an abiotic porphyrinogen in aqueous solution. Orig. Life Evol. Biosph. 39, 495–515. https://doi.org/10.1007/s11084-009-9168-3.
Lindsey, J.S., Chandrashaker, V., Taniguchi, M., Ptaszek, M., 2011. Abiotic formation of uroporphyrinogen and coproporphyrinogen from acyclic reactants. New J. Chem. 35, 65–75. https://doi.org/10.1039/C0NJ00716A.
Liu, L., Zheng, N., Yu, Y., Zheng, Z., Yao, H., 2024. Soil carbon and nitrogen cycles driven by iron redox: A review. Sci. Total Environ. 918.
Lubitz, L., Ogata, H., Rüdiger, O., Reijerse, E., 2014. Hydrogenases. Chem. Rev. 114, 4081–4148. https://doi.org/10.1021/cr4005814.
Ludwig, Kristin A., Shen, Chuan-Chou, Kelley, Deborah S., Hai Cheng, R., Edwards, Lawrence, 2011. U–Th systematics and 230Th ages of carbonate chimneys at the Lost City Hydrothermal Field. Geochimica et Cosmochimica Acta 75 (7), 1869–1888. https://doi.org/10.1016/j.gca.2011.01.008.
Ma, L., Pang, A.P., Luo, Y., Lu, X., Lin, F., 2020. Beneficial factors for biomineralization by ureolytic bacterium Sporosarcina pasteurii. Microbial Cell Factories 19, 12. https://doi.org/10.1186/s12934-020-1281-z.
Machado, A.L., Garnier, J., Ratié, G., Guimaraes, E., Monvoisin, G., Cloquet, C., Quantin, C., 2023. Nickel mass balance and isotopic records in a serpentinic weathering profile: implications on the continental Ni budget. Chemical Geology 634, 121586. https://doi.org/10.1016/j.chemgeo.2023.121586.
Maroney, M.J., Ciurli, S., 2014. Nonredox nickel enzymes. Chem. Rev. 114, 4206–4228. https://doi.org/10.1021/cr4004488.
Martin, W.F., 2020. Older than genes: the acetyl coa pathway and origins. Frontiers in Microbiology 11. Available at: https://www.frontiersin.org/articles/10.3389/fmicb.2020.00817.
Maurel, M.C., Ninio, J., 1987. Catalysis by a prebiotic nucleotide analog of histidine. Biochimie 69, 551–553.
Mayer, R.J., Kaur, H., Rauscher, S.A., Moran, J., 2021. Mechanistic insight into metal ion-catalyzed transamination. J. Am. Chem. Soc. 143, 19099–19111. https://doi.org/10.1021/jacs.1c08535.
Mazzei, L., Cianci, M., Benini, S., Ciurli, S., 2019. The structure of the elusive urease–urea complex unveils the mechanism of a paradigmatic nickel-dependent enzyme. Angew. Chem. Int. Ed. 58, 7415–7419. https://doi.org/10.1002/anie.201903565.
Mazzei, L., Musiani, F., Ciurli, S., 2020. The structure-based reaction mechanism of urease, a nickel dependent enzyme: tale of a long debate. J. Biol. Inorg. Chem. 25, 829–845. https://doi.org/10.1007/s00775-020-01808-w.
McCown, P.J., Corbino, K.A., Stav, S., Sherlock, M.E., Breaker, R.R., 2017. Riboswitch diversity and distribution. RNA 23, 995–1011. https://doi.org/10.1261/rna.061234.117.
Mével, C., 2003. Serpentinization of abyssal peridotites at mid-ocean ridges. Comptes Rendus Geosci. 335, 825–852. https://doi.org/10.1016/j.crte.2003.08.006.
Mielke, Randall E., Russell, Michael J., Wilson, Philip R., McGlynn, Shawn E., Coleman, Max, Kidd, Richard, Kanik, Isik, 2010. Design, Fabrication, and Test of a Hydrothermal Reactor for Origin-of-Life Experiments. Astrobiology 10 (8).
Mielke, R.E., Robinson, K.J., White, L.M., McGlynn, S.E., McEachern, K., Bhartia, R., Kanik, I., Russell, M.J., 2011. Iron-sulfide-bearing chimneys as potential catalytic energy traps at life's emergence. Astrobiol. 11, 1–18.
Miraula, M., Ciurli, S., Zambelli, B., 2015. Intrinsic disorder and metal binding in UreG proteins from Archae hyperthermophiles: GTPase enzymes involved in the activation of Ni(II) dependent urease. Journal of biological inorganic chemistry. JBIC Publ. Soc. Biol. Inorg. Chem. 20, 739–755. https://doi.org/10.1007/s00775-015-1261-7.
Miyazaki, Y., Oohora, K., Hayashi, T., 2022. Focusing on a nickel hydrocorphinoid in a protein matrix: methane generation by methyl-coenzyme M reductase with F430 cofactor and its models. Chem. Soc. Rev. 51, 1629–1639. https://doi.org/10.1039/D1CS00840D.
Mizuki, T., Kamekura, M., Dassarma, S., Fukushima, T., Usami, R., Yoshida, Y., Horikoshi, K., 2004. Ureases of extreme halophiles of the genus haloarcula with a unique structure of gene cluster. Biosci. biotechnol. biochem. 68, 397–406. https://doi.org/10.1271/bbb.68.397.
Moore, S.J., Sowa, S.T., Schuchardt, C., Deery, E., Lawrence, A.D., Ramos, J.V., Billig, S., Birkemeyer, C., Chivers, P.T., Howard, M.J., Rigby, S.E., Layer, G., Warren, M.J., 2017. Elucidation of the biosynthesis of the methane catalyst coenzyme F_{430}. Nature 543, 78–82. https://doi.org/10.1038/nature21427.
Moret, S., Dyson, P.J., Laurenczy, G., 2014. Direct synthesis of formic acid from carbon dioxide by hydrogenation in acidic media. Nat. Commun. 5, 4017. https://doi.org/10.1038/ncomms5017.
Muchowska, K.B., Varma, S.J., Moran, J., 2019. Synthesis and breakdown of universal metabolic precursors promoted by iron. Nature 569, 104–107. https://doi.org/10.1038/s41586-019-1151-1.
Musculus, F., 1876. Sur le ferment de l'urée. Comptes rendus de l'Académie des sciences 82, 333–336.
Naraoka, H., Yamashita, Y., Yamaguchi, M., Orthous-Daunay, F.-R., 2017. Molecular evolution of N-containing cyclic compounds in the parent body of the murchison meteorite. ACS Earth Space Chem. 1, 540–550. https://doi.org/10.1021/acsearthspacechem.7b00058.
Neubeck, A., Freund, F., 2020. Sulfur chemistry may have paved the way for evolution of antioxidants. Astrobiology 20 (5). https://doi.org/10.1089/ast.2019.2156.
Oba, Y., Takano, Y., Naraoka, H., Watanabe, N., Kouchi, A., 2019. Nucleobase synthesis in interstellar ices. Nat. Commun. 10, 4413.
Olson, K.R., Straub, K.D., 2008. The role of hydrogen sulfide in evolution and the evolution of hydrogen sulfide in metabolism and signaling. Physiology 31, 60–72. https://doi.org/10.1152/physiol.00024.2015.
Orgel, L.E., 2008. The implausibility of metabolic cycles on the prebiotic earth. PLOS Biol. 6, e18. https://doi.org/10.1371/journal.pbio.0060018.
Oró, J., Basile, B., Cortes, S., Shen, C., Yamrom, T., 1984. The prebiotic synthesis and catalytic role of imidazoles and other condensing agents. Orig. Life 14, 237–242. https://doi.org/10.1007/BF00933663.
Pantaleone, Stefano, Corno, Marta, Rimola, Albert, Balucani, Nadia, Ugliengo, Piero, 2022. The Journal of Physical Chemistry C 126 (4), 2243–2252. https://doi.org/10.1021/acs.jpcc.1c09947.
Parigi, Roberta, Pakostova, Eva, Reid, Joel W., Saurette, Emily M., McBeth, Joyce M., Ptacek, Carol J., Blowes, David W., 2022. Nickel isotope fractionation as an indicator

of Ni sulfide precipitation associated with microbially mediated sulfate reduction. Environ. Sci. Technol. 56, 7954–7962. https://doi.org/10.1021/acs.est.2c00523.
Pašava, J., Chrastný, V., Loukola-Ruskeeniemi, K., Šebek, O., 2019. Nickel isotopic variation in black shales from Bohemia, China, Canada, and Finland: a reconnaissance study. Mineral Deposita 54, 719–742.
Pasek, M., Lauretta, D., 2005. Aqueous corrosion of phosphide minerals from iron meteorites: A highly reactive source of prebiotic phosphorus on the surface of the early Earth. Astrobiol. 5, 515–535.
Pelmenschikov, V., 2006. Nickel superoxide dismutase reaction mechanism studied by hybrid density functional methods. J. Am. Chem. Soc. 128, 7466–7475. https://doi.org/10.1021/ja053665f.
Pereira, D.P.H., Leethaus, J., Beyazay, T., Vieira, A.N., Kleinermanns, K., Tüysüz, H., Martin, W.F., Preiner, M., 2022. Role of geochemical protoenzymes (geozymes) in primordial metabolism: specific abiotic hydride transfer by metals to the biological redox cofactor NAD+. FEBS J. 289, 3148–3162. https://doi.org/10.1111/febs.16329.
Peters, J.W., Schut, G.J., Boyd, E.S., Mulder, D.W., Shepard, E.M., Broderick, J.B., King, P.W., Adams, M.W.W., 2015. [FeFe]- and [NiFe]-hydrogenase diversity, mechanism, and maturation. Biochim. Biophys. Acta 1853, 1350. https://doi.org/10.1016/j.bbamcr.2014.11.021.
Preiner, M., Xavier, J.C., Sousa, F.L., Zimorski, V., Neubeck, A., Lang, S.Q., Greenwell, H. C., Kleinermanns, K., Tüysüz, H., McCollom, T.M., Holm, N.G., Martin, W.F., 2018. Serpentinization: connecting geochemistry, ancient metabolism and industrial hydrogenation. Life 8, 41. https://doi.org/10.3390/life8040041.
Preiner, M., Igarashi, K., Muchowska, K.B., Yu, M., Varma, S.J., Kleinermanns, K., Nobu, M.K., Kamagata, Y., Tüysüz, H., Moran, J., Martin, W.F., 2020. A hydrogen-dependent geochemical analogue of primordial carbon and energy metabolism. Nat. Ecol. Evol. 4, 534–542. https://doi.org/10.1038/s41559-020-1125-6.
Price, N.M., Morel, F.M.M., 1991. Colimitation of phytoplankton growth by nickel and nitrogen. Limnol. Oceanogr. 36 (6), 1071–1077. https://doi.org/10.4319/lo.1991.36.6.1071.
Ragsdale, S.W., 2007. Nickel and the carbon cycle. J. Inorg. Biochem. 101, 1657–1666. https://doi.org/10.1016/j.jinorgbio.2007.07.014.
Ragsdale, S.W., 2008. Enzymology of the Wood–Ljungdahl pathway of acetogenesis. Ann. N. Y. Acad. Sci. 1125, 129–136. https://doi.org/10.1196/annals.1419.015.
Ragsdale, S.W., 2009. Nickel-based enzyme systems. J. Biol. Chem. 284 (28), 18571–18575. https://doi.org/10.1074/jbc.R900020200.
Ragsdale, S.W., Pierce, E., 2008. Acetogenesis and the Wood–Ljungdahl pathway of CO2 fixation. Biochim. Biophys. Acta 1784, 1873–1898. https://doi.org/10.1016/j.bbapap.2008.08.012.
Ragsdale, S.W., Wood, H.G., Antholine, W.D., 1985. Evidence that an iron-nickel-carbon complex is formed by reaction of CO with the CO dehydrogenase from Clostridium thermoaceticum. Proc. Natl. Acad. Sci. USA 82, 6811–6814.
Ratié, G., Quantin, C., Maia De Freitas, A., Echevarria, G., Ponzevera, E., Garnier, J., 2019. The behavior of nickel isotopes at the biogeochemical interface between ultramafic soils and Ni accumulator species. Journal of Geochemical Exploration 196 (January), 182–191. https://doi.org/10.1016/j.gexplo.2018.10.008.
Raymond, J., Siefert, J.L., Staples, C.R., Blankenship, R.E., 2004. The natural history of nitrogen fixation. Mol. Biol. Evol. 21, 541–554. https://doi.org/10.1093/molbev/msh047.
Reeves, E.P., McDermott, J.M., Seewald, J.S., 2014. The origin of methanethiol in midocean ridge hydrothermal fluids. Proc. Nat. Acad. Sci. USA 111, 5474–5479. https://doi.org/10.1073/pnas.140064311.
Reissmann, S., Hochleitner, E., Wang, H., Paschos, A., Lottspeich, F., Glass, R.S., Böck, A., 2003. Taming of a poison: biosynthesis of the nife-hydrogenase cyanide ligands. Science 299, 1067–1070. https://doi.org/10.1126/science.1080972.
Ryabchuk, P., Agostini, G., Pohl, M.-M., Lund, H., Agapova, A., Junge, H., Junge, K., Beller, M., 2018. Intermetallic nickel silicide nanocatalyst—A non-noble metal–based general hydrogenation catalyst. Sci. Adv. 4, eaat0761. https://doi.org/10.1126/sciadv.aat07.
Sabatier, P., 1922. Catalysis in Organic Chemistry. D. van Nostand Company, New York, p. 15.
Sarah J., Selby, David, Cameron, Vyllinniskii, 2014. Characterising the nickel isotopic composition of organic-rich marine sediments. Chem. Geol. 387, 12–21. https://doi.org/10.1016/j.chemgeo.2014.07.017. ISSN 0009-2541.
Schoenmakers, L.L.J., Reydon, R., Kirschning, A., 2024. Evolution at the origins of life? Life 14, 175. https://doi.org/10.3390/life14020175.
Serganov, A., Patel, D.J., 2012. Metabolite recognition principles and molecular mechanisms underlying riboswitch function. Ann. Rev. Biophys. 41, 343–370. https://doi.org/10.1146/annurev-biophys-101211-113224.
Shalayel, I., Youssef-Saliba, S., Vazart, F., Ceccarelli, C., Bridoux, M., Vallée, Y., 2020. Cysteine Chemistry in Connection with Abiogenesis. Eur. J. Org. Chem. 3019–3023. https://doi.org/10.1002/ejoc.202000089.
Shearer, J., 2014. Insight into the structure and mechanism of nickel-containing superoxide dismutase derived from peptide-based mimics. Acc. Chem. Res. 47, 2332–2341. https://doi.org/10.1021/ar500060s.
Shen, C., Yang, L., Miller, S.L., Oró, J., 1987. Prebiotic synthesis of imidazole-4-acetaldehyde and histidine. Origins Life Evol. Biosph. 17, 295–305. https://doi.org/10.1007/BF02386469.
Shen, C., Yang, L., Miller, S.L., Oró, J., 1990a. Prebiotic synthesis of histidine. J. Mol. Evol. 31, 167–174. https://doi.org/10.1007/BF02109492.
Shen, C., Mills, T., Oró, J., 1990b. Prebiotic synthesis of histidyl-histidine. J. Mol. Evol. 31, 175–179. https://doi.org/10.1007/BF02109493.
Shen, C., Lazcano, A., Oró, J., 1990c. The enhancement activites of histidyl-histidine in some prebiotic reactions. J. Mol. Evol. 31, 445–452. https://doi.org/10.1007/BF02102070.
Sheng, Y., Abreu, I.A., Cabelli, D.E., Maroney, M.J., Miller, A.-F., Teixeira, M., Valentine, J.S., 2014. Superoxide dismutases and superoxide reductases. Chem. Rev. 114, 3854–3918. https://doi.org/10.1021/cr4005296.
Sherwood, A.V., Henkin, T.M., 2016. Riboswitch-mediated gene regulation: novel RNA architectures dictate gene expression responses. Ann. Rev. Microbiol. 70, 361–374. https://doi.org/10.1146/annurev-micro-091014-104306.
Siegbahn, P.E.M., Chen, S.-L., Liao, R.-Z., 2019. Theoretical studies of nickel-dependent enzymes. Inorganics 2019 (7), 95. https://doi.org/10.3390/inorganics7080095.
Sleep, N.H., Meibom, A., Fridriksson, T., Coleman, R.G., Bird, D.K., 2004. H2-rich fluids from serpentinization: geochemical and biotic implications. Proc. Natl Acad. Sci. USA 101, 12818–12823. https://doi.org/10.1073/pnas.04052891.
Soares, A.R.M., Taniguchi, M., Chandrashaker, V., Lindsey, J.S., 2012. Self-organization of tetrapyrrole constituents to give a photoactive protocell. Chem. Sci. 3, 1963–1974. https://doi.org/10.1039/C2SC01120D.
Soares, A.R.M., Taniguchi, M., Chandrashaker, V., Lindsey, J.S., 2013a. Expanded combinatorial formation of porphyrin macrocycles in aqueous solution containing vesicles. A prebiotic model. New J. Chem. 37, 1073–1086. https://doi.org/10.1039/C3NJ41041B.
Soares, A.R.M., Anderson, D.R., Chandrashaker, V., Lindsey, J.S., 2013b. Catalytic diversification upon metal scavenging in a prebiotic model for formation of tetrapyrrole macrocycles. New J. Chem. 37, 2716–2732. https://doi.org/10.1039/C3NJ00498H.
Sorensen, Jeffry V., Gueguen, Bleuenn, Stewart, Brandy D., Peña, Jasquelin, Rouxel, Olivier, Toner, Brandy M., 2020. Large nickel isotope fractionation caused by surface complexation reactions with hexagonal birnessite. Chemical Geology 537, 119481. https://doi.org/10.1016/j.chemgeo.2020.119481. ISSN 0009-2541.
Spivak-Birndorf, L.J., Wang, S.-J., Bish, D.L., Wasylenki, L.E., 2018. Nickel isotope fractionation during continental weathering. Chemical Geology 476, 316–326. https://doi.org/10.1016/j.chemgeo.2017.11.028.
Stüeken, E.E., Kipp, Michael A., Koehler, M.A., Buick, M.C., 2016. The evolution of Earth's biogeochemical nitrogen cycle. Earth Sci. Rev. 160, 220–239. https://doi.org/10.1016/j.earscirev.2016.07.007.
Sung, H.-L., Nesbitt, D.J., 2020. Sequential folding of the nickel/cobalt riboswitch is facilitated by a conformational intermediate: insights from single-molecule kinetics and thermodynamics. J. Phys. Chem. B 124 (34), 7348–7360. https://doi.org/10.1021/acs.jpcb.0c05625.
Thauer, R.K., 1998. Biochemistry of methanogenesis: a tribute to Marjory Stephenson: 1998 Marjory Stephenson Prize Lecture. Microbiology 144, 2377–2406. https://doi.org/10.1099/00221287-144-9-2377.
Thornalley, P.J., 1993. The glyoxalase system in health and disease. Mol. Aspects Med. 14, 287–371. https://doi.org/10.1016/0098-2997(93)90002-U.
Timm, J.D., Pike, D.H., Mancini, J.A., Tyryshkin, A.M., Poudel, S., Siess, J.A., Molinaro, P.M., McCann, J.J., Waldie, K.M., Koder, R.L., Falkowski, P.G., Nanda, V., 2023. Design of a minimal di-nickel hydrogenase peptide. Sci. Adv. 9, eabq1990. https://doi.org/10.1126/sciadv.abq199.
Türke, N., 2015. Stability constants of mixed ligand complexes of nickel(II) with adenine and some amino acids. Bioinorg. Chem. Appl. 374782. https://doi.org/10.1155/2015/374782.
Vance, D., Archer, C., Bermin, J., Perkins, J., Statham, P.J., Lohan, M.C., Ellwood, M.J., Mills, R.A., 2008. The copper isotope geochemistry of rivers and the oceans. Earth Planet. Sci. Lett. 274, 204–213. https://doi.org/10.1016/j.epsl.2008.07.026.
Vance, D., Little, S.H., Archer, C., Cameron, V., Andersen, M.B., Rijkenberg, M.J.A., Lyons, T.W., 2016. The oceanic budgets of nickel and zinc isotopes: the importance of sulfidic environments as illustrated by the Black Sea. Philos. Transact. R. Soc. A Math. Phys. Eng. Sci. 374, 20150294. https://doi.org/10.1098/rsta.2015.0294.
Varma, S.J., Muchowska, K.B., Chatelain, P., Moran, J., 2018. Native iron reduces CO_2 to intermediates and end-products of the acetyl-CoA pathway. Nat. Ecol. Evol. 2, 1019–1024. https://doi.org/10.1038/s41559-018-0542-2.
Vignais, P.M., Billoud, B., 2017. Occurrence, classification, and biological function of hydrogenases: an overview. Chem. Rev. 107, 4206–4272. https://doi.org/10.1021/cr050196r.
Wächtershäuser, G., 1988. Before enzymes and templates: theory of surface metabolism. Microbiol. Mol. Biol. Rev. 52, 452–484. https://doi.org/10.1128/mr.52.4.452-484.1988.
Walsh, C.T., Orme-Johnson, W.H., 1987. Nickel enzymes. Biochemistry 26, 4901–4906. https://doi.org/10.1021/bi00390a001.
Wang, S.-J., Wasylenki, L.E., 2017. Experimental constraints on reconstruction of archean seawater Ni isotopic composition from banded iron formations. Geochimica et Cosmochimica Acta 206, 137–150. https://doi.org/10.1016/j.gca.2017.02.023.
Wang, S., Lee, M.H., Hausinger, R.P., Clark, P.A., Wilcox, D.E., Scott, R.A., 1994. Structure of the dinuclear active site of urease. X-ray absorption spectroscopic study of native and 2-mercaptoethanol-inhibited bacterial and plant enzymes. Inorg. Chem. 33, 1589–1593. https://doi.org/10.1021/ic00086a006.
Wang, S.J., Wang, W., Zhu, J.M., Wu, Z., Liu, J., Han, G., Teng, F.Z., Huang, S., Wu, H., Wang, Y., Wu, G., Li, W., 2021. Nickel isotopic evidence for late-stage accretion of Mercury-like differentiated planetary embryos. Nat Commun. 12 (1), 294. https://doi.org/10.1038/s41467-020-20525-1. PMID: 33436633; PMCID: PMC7803775.
Wang, W.-J., Wie, W.-J., Liao, R.-Z., 2018. Deciphering the chemoselectivity of nickel-dependent quercetin 2,4-dioxygenase. Phys. Chem. Chem. Phys. 20, 15784. https://doi.org/10.1039/C8CP02683A.
Wasylenki, L.E., Howe, H.D., Spivak-Birndorf, L.J., Bish, D.L., 2015. Ni isotopefractionation during sorption to ferrihydrite: Implications for Ni in banded iron formations. Chem. Geol. 400 (0), 56–64.
Weiss, M.C., Sousa, F.L., Mrnjavac, N., Neukirchen, S., Roettger, M., Nelson-Sathi, S., Martin, W.F., 2016. The physiology and habitat of the last universal common

ancestor. Nat. Microbiol. number 16116. https://doi.org/10.1038/nmicrobiol.2016.116.
White, D.H., Erickson, J.C., 1980. Catalysis of peptide bond formation by histidyl-histidine in a fluctuating clay environment. J. Mol. Evol. 16, 279–290. https://doi.org/10.1007/BF01804979.
Williams, R.J.P., 1997. The natural selection of the chemical elements. Cell. Mol. Life sci. 53, 816–829. https://doi.org/10.1007/s000180050102.
Wooldridge, S.A., 2008. Mass extinctions past and present: a unifying hypothesis. Biogeosci. Dis. 5, 2401–2423. https://doi.org/10.5194/bgd-5-2401-2008.
Yadav, G.D., Kharkara, M.R., 1995. Liquid-phase hydrogenation of saturated and unsaturated nitriles: activities and selectivities of bimetallic nickel-copper and nickel-iron catalysts supported on silica. Appl. Catal. A Gen. 126, 115–123. https://doi.org/10.1016/0926-860X(95)00039-9.
Yanai, I., Wolf, Y.I., Koonin, E., 2002. Evolution of gene fusions: horizontal transfer versus independent events. Genome Biol. 3 (2002). https://doi.org/10.1186/gb-2002-3-5-research0024.
Ye, S., Wu, X.A., Wie, L., Tang, D., Sun, P., Bartlam, M., Rao, Z., 2007. An insight into the mechanism of human cysteine dioxygenase. Key roles of the thioether-bonded tyrosine-cysteine cofactor. J. Biol. Chem. 282, 3391–3402. https://doi.org/10.1074/jbc.M609337200.
Zamble, D.B., Li, Y., 2009. Nickel homeostasis and nickel regulation: an overview. Chem. Rev. 109, 4617–4643. https://doi.org/10.1021/cr900010n.
Zheng, K.Y., Ngo, P.D., Owens, V.L., Yang, X.P., Mansoorabadi, S.O., 2016. The biosynthetic pathway of coenzyme F430 in methanogenic and methanotrophic archaea. Science 354, 339–342. https://doi.org/10.1126/science.aag2947.